Chapter one

1.1Introduction

Ultrasound was discovered as long ago as 1880s.the French Physicist Pierre and their collogue discovered the piezoelectric effect and attempted to develop Piezoelectric materials as senders and receivers of high frequency mechanical disturbance (ultrasound wave) through materials and the industrial use of ultrasound began in 1928s with suggestion of soviet physicist Sokolov, that it could be used to detect flow in materials (Hendee, 2002). The primary of ultrasonic imaging to date has been that of pulse echo mode the principle is very similar to that of sonar In essence, following an ultrasound pulse transmission echoes from median interacted with the object and reflection waves use to build up and construct a picture of the object (Hendee, 2002).

Potential of Ultrasound as an imaging modality was realized as early as the late 1940s, when utilizing sonar and Radar technology during the World War II, finding become practical during the Second World War following the loss of the Titanic. Medical use of ultrasound through the 1930s were confined to therapeutic application such as cancer treatment and physical therapy for various ailments .and several group investigators around the world started exploring diagnostic capabilities of Ultrasound (Goldberg,1989) . In early 1950, John wild and John Ried in Minnesota developed a prototype B-mode ultrasonic imaging instrument and were able to demonstrate the capability of ultrasound for imaging and characterizing a cancerous tissue at frequency as high as 15 MHz.And medical diagnostic technology became a widely accepted as diagnostic tool in early 1970sJohn Wild,s pioneering effort and accomplishment were recognized with the Japan Prize In 1991. At the same time apparently unaware of the effort by wild and Reids, Douglas Howry and Joseph of Colorado and Denva also built and ultrasonic imaging device

with which they produced across-sectional image of the arm and leg. (Ki kirk shug 2006)

Starting in the late 1940s medical application of ultrasound in Japan were explored by Kenji Tanaka and Toshio wagai were credited with earliest development of ultrasonic Doppler device for monitoring tissue motion and blood flow in 1955. Today ultrasound is the second most utilized diagnostic imaging modality in medicine and is a critically important tool of any medical application. (K.Kirk Shung2006)

In the 1950's Professor Iain Donald, then Regius Professor of Midwifery at Glascgow University pioneered Ultrasonography use in obstetrics. (AsimKurjak 2006). Then become the most useful imaging modality in obstetrics.

Ultrasound continues to be one of the most important diagnostic tools witch used by a wide range of healthcare professional across many applications. Ultrasounds not only complement the more traditional approaches such as X-Ray, but also possess unique characteristics that are advantage in comparison to other competing modalities such as X-Ray, computed Tomography (CT), Radionuclide emission tomography, and Magnetic Resonance Imaging.

Ultrasound is the tool of choice in obstetric primarily because of the following advantages (Jan A batesl 2004) as well as (K.KirkShung 2006).

- It is a form of non-ionizing radiation and is considered safe to the best of present knowledge
- It is less expensive.

- It Produces image in real time.
- It has resolution in the millimeters range for frequencies being clinically used to day which may be improved if the frequency is increased
- It can yield blood flow information by applying Doppler principle
- It is portable and thus can easily to be transported to the bedside of a patient.

But Ultrasound also has several drawbacks and limitation such as

- Organs containing gasses and bone structures cannot be adequately visualized
- Only a imitated window is available for ultrasonic examination of certain organs such as heart, and neonatal brain.
- It depends on operator skills.

It is sometimes impossible to obtain good images from certain type of patient including obese patients (Jan A bates 2004)

The many advantages of ultrasound that it can be a valuable diagnostic tool in many medical disciplines as cardiology, Gynecology, pediatrics, Radiology, surgery, Neurology. (Jan A bates 2004).

Urinary system is also known as excretory system of human body. It is the system of production, storage and elimination of urine. Formation and elimination of urine is important for human body because urine contains nitrogenous wastes of the body that must be eliminated to maintain homeostasis. Nitrogenous wastes are formed by metabolic activities in the cells. These nitrogenous wastes along with excess of salts and water are combined in the kidneys to form urine. Urinary system is important for keeping the internal environment of the body clean. Urinary system maintains proper homeostasis of water, salts and nitrogenous wastes.

Kidneys are the major organs of urinary system. Formation of urine takes place in kidneys which are two bean shaped organs lying close to the lumbar spine, one on each side of the body. Knowledge of kidney character is important for clinical assessment of renal disease. This study were to establish a normal range of values for kidney length and volume in normal Sudanese adults with no known history of renal disease and determine the usefulness of body mass index (BMI),body surface area (BSA), Glomerular filtration rate (GFR), Total body water (TBW),Creatinin Clearance (CrCl), Serum Creatinin Level (SrCr) for prediction of kidney characters. On the other hand touched this study to characterization of normal renal tissues in MRI images for Sudanese population using texture analysis. The renal tissues were classified into three classes as, cortex, medulla and pelvis using SGLD matrix(S.Snell, 2007)..

1-2Problem of study

The variable renal tests usually may not be sufficient to give the exact diagnosis of renal problems (e.g. glomerulonephritis and pyelonephritis) ,so recognizing the echo pattern images using image processing technique in addition to ultrasound characteristics might solve the problem and hence save the time and assure quality of diagnosis.

1-3Objectives:

1.3.1General objective:

- To characterize the renal tissues as normal, glomerulonephritis or pyelonephritis renal tissues ultrasonographically and by image processing methods

Specific objectives:

- To assess renal size and texture feature.
- To determine the characteristic of image pattern of glomerulonephritis and pyelonephritis.
- To determine the normal image pattern of kidneys in normal patients
- To classify the kidneys into normal, glomerulonephritis and pyelonephritis using linear discriminant analysis.
- To generate linear equations that can be used in routine work for renal classification.

1-4Over view of study

This study falls into five chapters with chapter one is an introduction, which include introductory notes on renal and texture analysis, as well as statement of the problem and study objectives. While Chapter two included a comprehensive scholarly literature reviews concerning the previous studies. Chapter three deals with the methodology, where it provides an outline of material and methods used to acquire the data in this study as well as the method of analysis approach. While the results were presented in chapter four, and finally Chapter five include discussion of results, conclusion and recommendation followed by references and appendices.

Chapter two

Background and Literature review

Urinary system consist of two kidneys lie on the posterior abdominal wall; two ureter, which run down on the posterior abdominal wall and enter the pelvis ; one urinary bladder located within the pelvis; and one urethra, which passes through the perineum. (Snell, 2007).

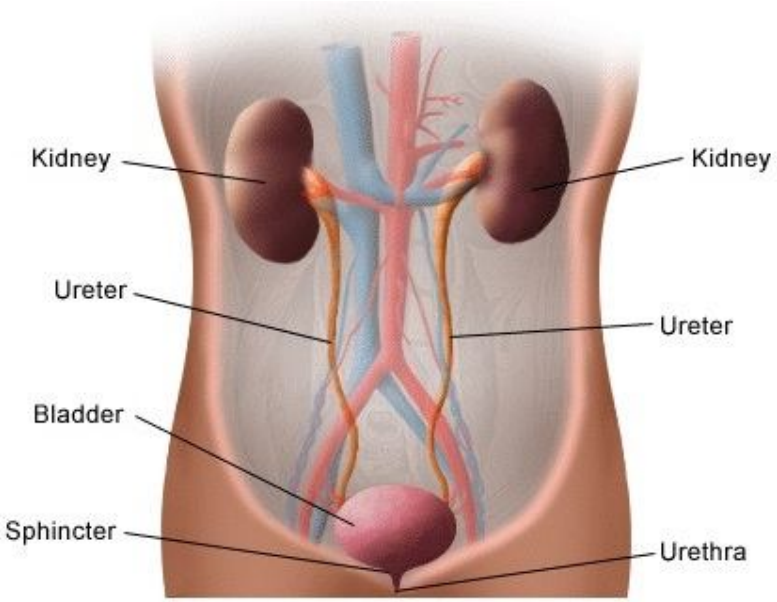

Figure.(2-1) Front view of urinary tract (Snell, 2007).

2.1Anatomy :

The two kidneys are situated behind the peritoneum upper on the posterior abdominal wall on each side of the vertebral column: they are largely under cover of the costal margin. Each kidney has a dark brown

outer cortex and a light brown inner medulla. the medulla is composed of about a dozen renal pyramids , each having its base oriented toward the cortex and its apex , the renal papilla , projecting medially .the cortex extends into the medulla between adjacent pyramids as the renal columns .extending from the bases of renal pyramids into the cortex are striations known as medullary rays. (Snell, 2005)**.**

The renal sinus, which is the space within the hilum, contains the upper expanded end of the ureter, the renal pelvis. This divides into two or three major calyces, each of which divides in to two or three minor calyces. Each minor calyx is indented by the apex of renal pyramid, the renal papilla.(Snell, 2005)**.**

The left kidney usually lies 1 to 2 cm higher than the right kidney. The kidneys are mobile and will move depending on body position. In the supine position, the superior pole of the left kidney is at the level of the 12^{th} thoracic vertebra, and the inferior pole is at the level of the third lumbar vertebra.(Snell, 2005)

2.1.1General Structure ofthe Kidneys

A fibrous tissue capsule which is backer to the renal parenchyma. The capsule provides a specular interface and is well demonstrated on the position of the kidneys which are located at right angles to the central axis of the sound beam.(Harold, 2006).).

The renal parenchyma is divided into the cortex and the medulla. The renal cortex is the outer part of the parenchyma and contains the functional units of the kidney called the nephrons. Columns of renal parenchyma extend centrally between the renal pyramids. The renal columns are also known as the septal cortex or the columns of Bertin. The columns contain the interlobar arteries and veins.(Harold, 2006).).

The renal medulla consists of renal pyramids. The bases of the pyramids are directed toward the cortex and the apices of the pyramids converge toward the renal sinus. The apices form pointed processes called papillae. The papillae protrude into minor calyces which are cup-shaped structures that drain into a major calyx. Multiple major calyces drain into the renal pelvis.(Harold, 2006).).

The pyramids consist of collecting tubules+ which convey urine from the nephrons into the minor calyces.

The collecting system of the kidney consists of the renal pelvis which divides within the renal sinus into 2-3 large branches called major calyces. Each major calyx divides into several short branches called minor calyces. The expanded end of each minor calyx is moulded around 1-3 renal papillae. The major calyces are demonstrated on scans as fine extensions from the pelvis which end in cup-shaped structures near the apices of the pyramids. The major calyces are often referred to as the infundibula (singular - infundibulum).(Harold, 2006).

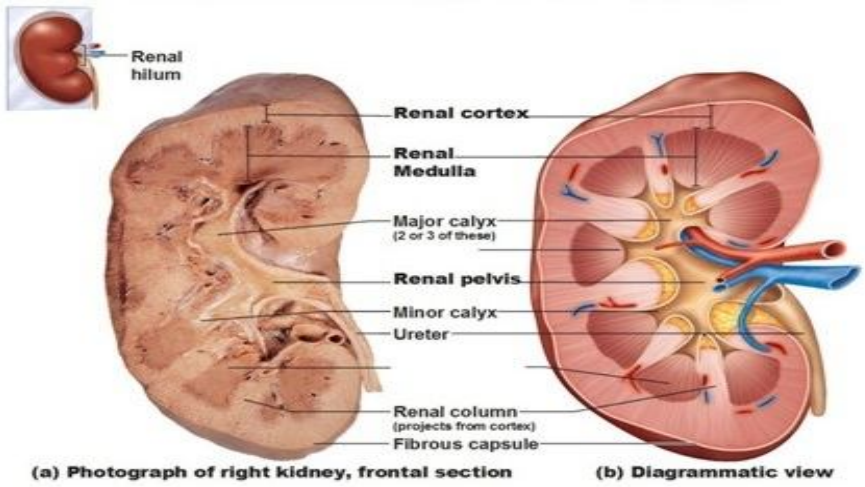

Figure. (2-2)internal gross anatomy of the kidneys(Harold, 2006).

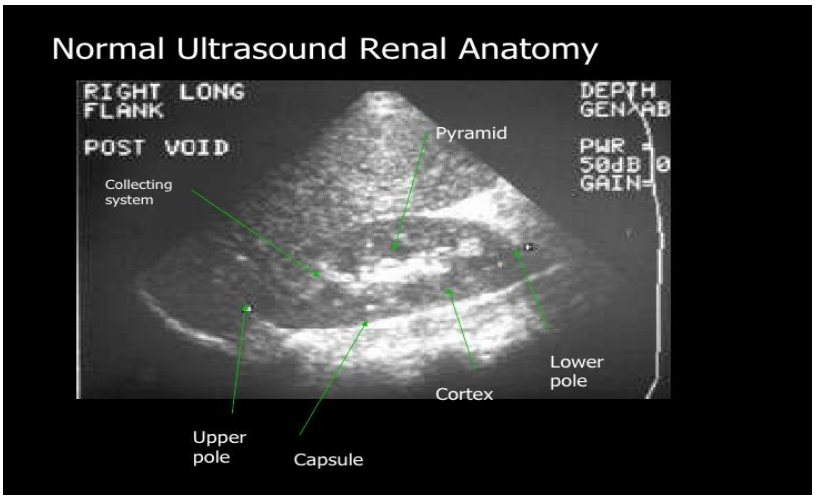

Figure. (2-3) Normal ultrasound renal anatomy

2.1.2Blood supply:

The renal artery arises from the aorta at the level of the second lumber vertebra. Each renal artery usually divides into five segmental arteries that enter the hilum of kidney, four in frontal and one behind the renal pelvis. They are distributed to different segments or areas of the kidney. Lobar arteries arise from each segmental artery. One for each renal pyramid. Before entering the renal substance, each lobar artery gives off two or three interlobar arteries .the interlobar arteries run toward the cortex on each side of the renal pyramid. At the junction of the cortex and the medulla, the interlobar arteries give off the actuate arteries, which arch over the bases of the pyramid .the actuate arteries give off several interlobular arteries that ascend in the cortex; the afferent glomerular arteries arise as branches of the interlobular arteries. The renal vein emerges from the hilum in front of the renal artery and drains into the inferior vena cava. (Snell, 2005)**.**

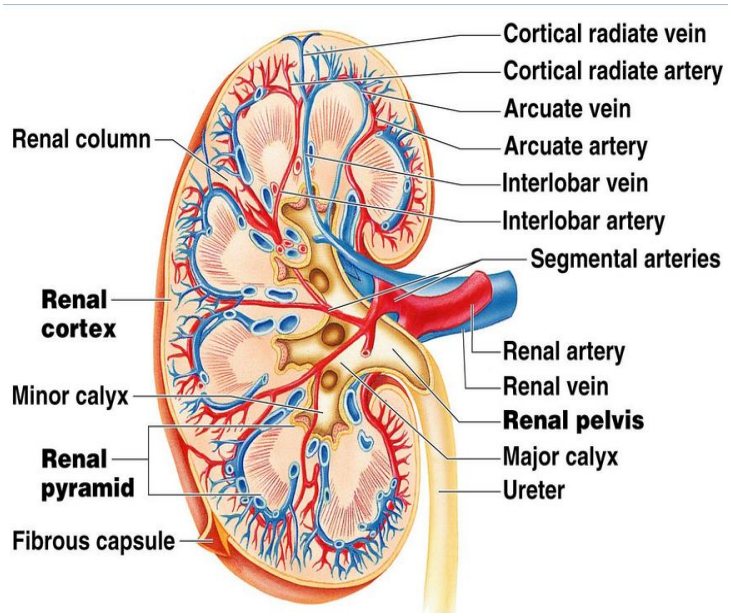

Figure . (2-4)Blood supply of the kidney(Tortora, 2012)

2.1.3Nerve supply :

Renal sympathetic plexus. The afferent fibers that travel through the renal plexus enter the spinal cord in the tenth eleventh, and twelfth thoracic nerves. (McMinn, 2009)**.**

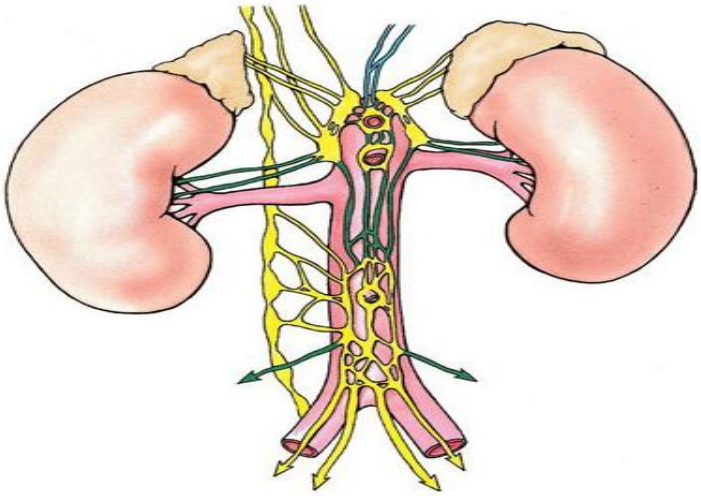

Figure. (2-5) Nerve supply of the kidney(McMinn, 2009)**.**

2.2 Physiology of kidneys:

The two kidneys function to excrete most of the waste products of metabolism. They play major role in controlling the water and electrolyte balance within the body and in maintaining the acid-base balance of the blood. The waste products leave the kidneys as urine, which passes down the ureter to the urinary bladder, located within the pelvis. The urine leaves the body in the urethra. .(Tortora, 2012).

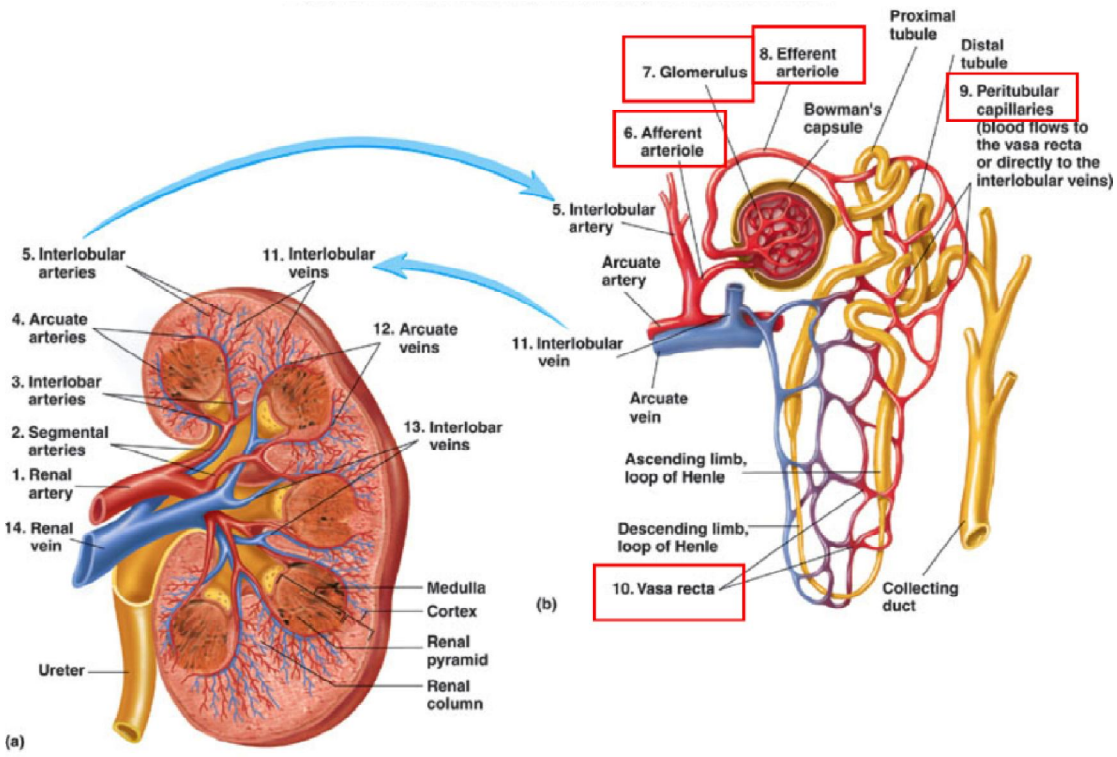

Figure. (2-6) Function of the kidney.(Tortora, 2012).

2.2.1 Glomerular filtration

Average values for mythical 70 kg male

GFR ~ 180 l/d ~ 125 ml/minthis represents ~ 20% of plasma entering the glomerular capillaries

Total plasma volume ~ 3.0 l filtered ~ 60 times/day

urine production ~ 1-2 l/d ~ 99% of filtrate is reabsorbed Composition of Filtratethe filtration barrier is freely permeable to water and crystalloids, MW 30,000, however, is virtually impermeable to colloids small quantities, mainly of albumin scape ~ 50 mg/las proteins are not filtered, the filtrate electrolyte concentrations vary slightly from plasma water. .(Tortora, 2012).

2.3 Pathology of Kidneys:

The kidney disease is generally divided into two types of congenital and acquired, congenital diseases such as renal agenesis {solitary kidney}, Ectopic kidney, Horse shoe kidney, Cross ectopic, Duplication of ureter and renal pelvis. Acquired diseases such as Stones, Inflammatory diseases, Kidney masses, renal hypertension, renal obstruction and Vesicorectal.(Kemp, 2008).

Most of this disease affects the size of the kidney, while other may likely to change in the renal tissue i.e. (cortex, medulla and pelviocalyceal system) (Kemp, 2008)

2.3.1 Simple Renal Cysts:

These are true cysts that have a serious epithelial lining and are fluid filled, benigncortical masses. They meet all the ultrasound criteria of a simple cyst: they arespherical, anechoic, and thin-walled and have accentuated posterior enhancement.

Sonographic Appearances - These lesions range in size from a few millimeters toseveral centimeters. they are most frequently unilocular; are rarely symptomatic and even when multiple are of no major clinical significance. Someauthors feel simple cortical cysts are benign degenerative manifestations of renalaging. “One-half of all adults older than age 50 have simple renal cysts.(Buirwin,2002).

2.3.2 Multisystem Dysplastic Kidney

It is a congenital, nonhereditary, cystic renal disease. It is the most common cause of a palpable abdominal mass in a newborn. MCDK is typically unilateral, affecting a single kidney in its entirety, but may be bilateral or segmental. The IVP and nuclear medicine scan would indicate absence of function. Dean (D. Buirwin,2002).

Sonographic Appearances - Characteristically, the kidney is large and filled withcysts of various sizes. The cysts do not communicate and appear benign. There is no evidence of renal parenchyma, pelvis or ureter. (Buirwin,2002).

2.3.3Calyceal Diverticulum

This is an out pouching from the calyx. Stasis of urine may occur predisposing thepatient to infection and stone formation. The diverticulum can project into the renalparenchyma. (Buirwin,2002)

2.3.4 Hydronephrosis

Hydronephrosis refers to dilatation of the renal collecting system most frequently causedby incomplete or complete obstruction. Hydro ureter is dilatation of the ureter also causedby complete or incomplete obstruction. (D. Buirwin,2002)

Causes - In infants and children ureteropelvic junction obstruction, posterior urethralvalves in males and Prune Belly Syndrome are the most common causes of obstruction.Calculi is the most common cause in adults followed by tumors of the kidney, ureter andbladder. Less common causes are inflammatory ureteral strictures, neurogenic bladder andbladder outlet obstruction by Prune Belly Syndrome, aureteropelvic junction obstruction, Posterior urethral valves and vesicoureteral reflux (VUR). (D. Buirwin,2002)

2.3.5 Renal Calculus Disease

Urolithiasisis most prevalent in male's aged 20-40 years.1 Calculi can form in any part ofthe urinary tract but most form in the kidneys. They may be clinically silent or associatedwith flank pain. Hematuria (gross or microscopic) and renal colic are most often associatedwith ureteric calculi. Stones can occur within any part of the kidneys - the renal cortex,medulla, vessels, calyces or renal pelvis. Most calculi arise in the collecting system. Stoneformation may be idiopathic1 or associated with stasis (stagnation) of urine, prolongeddigestion of stone forming substances, chronic urinary infections and climate conditionsassociated with dehydration.5 Stasis also predisposes the patient to infection. Ultrasounddemonstrates calculi as highly echogenic structures regardless of chemical compositionShadow detection posterior to the stone depends on stone size, transducer frequency, andtransducer focal zone. Tiny calculi will not shadow if they are smaller than the focal zone. (D. Buirwin,2002)

2.3.6Neoplasms

2.3.6.1 Benign Lesions

Angiomyolipoma (AML)

It is a benign solid tumor containing variable amounts of blood vessels (angio), smoothmuscle (myo) and fat (lipoma).The sonographic appearances depend upon the predominance of one of the threecomponents. Typically, AMLs are extremely hyperechoic indicating the predominance offathowever, if muscle or vascular components predominate the lesion may be hypoechoic.Shadowing is demonstrated in 33% of AMLs. (D. Buirwin,2002)

Oncocytoma

Oncocytoma is a benign solid renal tumor occurring most often in men in their 60's. It isusually asymptomatic and an incidental finding.Sonographically, the tumor is solid, homogeneous and generates low levels ofechogenicity. A stellate central hyperechoic scar is seen in about 25% of cases and thenonly in lesions greater than 3 cm.2 However, “no imaging finding reliably distinguishes thistumor from renal cell carcinoma. Diagnosis is made by surgical excision or biopsy. (D. Buirwin, 2002)

2.3.6.2 Malignant Lesions

Renal Cell Carcinoma (RCC)

This is a primary tumor of the renal parenchyma thought to originate from the renal tubularepithelium. It is also called a hypernephroma or a renal adenocarcinoma. Renal cell carcinomas (RCC) are the most common primary malignant renal parenchymaltumors (86%) These tumors occur most frequently in males between the fifth to theseventh decade. They are usually unilateral and clinically silent until they become large.(D. Buirwin,2002).

Sonographically appears as

Characteristically, a spherical, solitary, unilateral tumor of variable size and echogenicity. The majority of tumors are either isoechoic or hypoechoic to the normal renal parenchyma, however 10% are more echogenic than normal renal parenchyma. (D. Buirwin,2002)

Calcification is common (up to 18%) and variable in appearance: punctate, coarse,central, peripheral or curvilinear. (D. Buirwin,2002)

The mass frequently distorts the collecting system .Hydronephrosis is not a commonfeature.

RCC is a non-encapsulatedtumor; therefore the borders are poorly defined. Tumorsare often exophytic (D. Buirwin,2002)..

Cystic forms of RCC most often have thick walls and internal debris. RCC arisingwithin simple cysts are rare and appear as cysts with a mural nodule.

Multicystic form of RCC has thick walls (>2mm) and thick septations.

Metastasis - Metastatic lymphadenopathy is usually near the renal vessels andaround and between the IVC and aorta.1,2 Hepatic metastasis may be by

direct extension or hematogenous spread. hepatic metastases have variableappearances. (D. Buirwin,2002)

Transitional Cell Carcinoma (TCC)

This is a malignancy involving the epithelial lining of the renal collecting system, ureters orbladder. It usually occurs in older age groups between 50 to 70, with a higher incidence inmales.Most renal TCCs develop in the renal pelvis or major calyces and produce mass lesionswithin the renal sinus. TCC may occasionally infiltrate the renal parenchyma focally ordiffusely causing enlargement of the kidney and loss of function (without the presence ofa discrete mass). (D. Buirwin,2002).

The ultrasound appearances of a renal pelvic TCC are characteristically those of a solid,homogeneous, hypoechoic or isoechoic mass centrally located within the renal sinus. Itcauses a separation of the central echo complex. (D. Buirwin,2002)

Renal Lymphoma

The kidney does not contain lymphoid tissue, therefore lymphomatous involvement of thekidney is metastatic in origin and occurs by hematogenousdissemination or directextension of retroperitoneal disease.Renal involvement is common with Non-Hodgkin's lymphoma and less common withHodgkin's lymphoma. The disease is usually widespread by the time renal involvement isevident. Most patients have no urinary symptoms. (D. Buirwin,2002).

Sonographic Appearances as

Focal parenchymal involvement, which is most common (60%),consists of multiple, small (1-3 cm), bilateral, solid, homogeneous, hypoechoic tumors.

Direct invasion (25-30%) into the renal sinus from retroperitoneal lymph nodemasses is typically nodular, hypoechoic and homogeneous. The mass maycause hydronephrosis. (D. Buirwin,2002)

A solitary homogeneous, hypovascular solid mass may be seen in 10-20% of

renal lymphomas.1 They can become large - 15 cm in size and beindistinguishable sonographically from RCC.

Diffuse infiltration globally enlarges the kidney with minimum or no alterationin the shape. Invasion of the renal sinus results in the loss of the echogeniccentral echo complex. (D. Buirwin,2002).

Perirenal involvement occurs when the disease invades the perirenal space and surrounds the kidney. The kidney may not be directly involved. This appears as a hypoechoic mass or rind partially or completely surrounding the kidney.

This pattern of involvement is virtually pathognomonic of lymphoma, but is uncommon. The appearances may be confused with hematoma in the perirenalspace. (D. Buirwin,2002)

Renal Leukemia:

Lymphoma and leukemia have a predilection for infiltration of the renal parenchyma andoften cause focal or diffuse renal enlargement.“Acute lymphoblastic leukemia is the mostcommon form to involve the kidney.(D. Buirwin,2002)

Sonographically, diffuse, bilateral renal enlargement is most common1 with loss of corticomedullary definition. The parenchyma may have increased or

decreased echogenicity. There may be distortion of the central echo complex.(D. Buirwin,2002)

Nephroblastoma

A nephroblastoma is a rapidly growing malignant tumor of the kidneys, consisting ofembryonal elements. It is also known as Wilm's tumors, Wilm'sembryoma or embryonal carcinoma

A nephroblastoma is the most common renal tumor in children. It is seen mostcommonly in children between 2 to 3 years of age.

Sonographically a Wilm's tumor is characteristically a large, intrarenal, solid mass with awell-defined margin or pseudocapsule of fibrous tissue and compressed renal parenchyma..(D. Buirwin,2002)

The tumor may be homogeneous or heterogeneous, if necrosis or hemorrhage hasoccurred. “The tumor rarely is calcified, rarely crosses midline, and rarely envelopes majorblood vessels, such as the aorta or IVC.An adrenal neuroblastoma, common to a similarage group, does cross midline, has calcifications in half the cases and does envelope blood vessels.(D. Buirwin,2002)

Metastases to the kidney

Metastases to the kidney are usually asymptomatic and demonstrated in patients with aknown malignancy which has already metastasized elsewhere. Spread to the kidneys is viathe hematogeneous route. The most common primary tumors associated with renalmetastases are from the lung, breast and RCC of the contralateral kidney. Less commonare colon, stomach, cervix, ovary, pancreas and prostate primaries..(D. Buirwin,2002)

The sonographic appearance of renal metastases is nonspecific:

Diffuse infiltration is demonstrated as renal enlargement with distortion of normalarchitecture and loss of normal corticomedullary definition.

Multiple metastases are small, hypoechoic, poorly marginated masses resemblinglymphomas.(D. Buirwin,2002)

A solitary metastasis is identical to a RCC. This often occurs with a primary from a colon carcinoma. A biopsy is required for a definitive diagnosis.(D. Buirwin,2002)

2.3.7 Acute Renal Failure (ARF)

Renal failure is considered acute if it develops over days or weeks, andchronic if it spans months or years. Acute or chronic renal failure may result from insufficient renal perfusion(prerenal causes), intrinsic renal disease (renal causes), or obstructive uropathy (postrenalcauses). In the setting of ARF, the main purpose of the US study is to excludehydronephrosis.(D. Buirwin,2002)

Causes:

Acute tubular necrosis (ATN) is the most common medical renal disease to cause acute reversible renal failure. ATN is the result of ischemia due to major trauma, massive hemorrhage (hypotension), dehydration, heavy metal exposure and chemicals toxic to the kidneys.

Sonographically the kidneys may be normal or enlarged with cortical echogenicity and prominent, hypoechoic pyramids.

Acute Glomerulonephritis is a disease of the renal glomeruli associated with various systemic diseases such, as lupus erythematosus. Patients present with hematuria, hypertension and azotemia.

Sonographically, “both kidneys are affected and the size may range from normal to markedly enlarged. The echo pattern of the cortex is altered with medullary sparing and may be normal, hypoechoic or hyperechoic. with treatment the kidneys revert to normal size and echo pattern.

Acute Interstitial Nephritis is an acute hypersensitivity reaction of the kidney often

Related to drugs such as, penicillin, non-steroidal anti-inflammatory drugs and furosemide. Renal failure resolves when drug use is suspended.

Sonographically there are enlarged hyperechoic kidneys.(D. Buirwin,2002)

2.3.8 Chronic Renal Failure (CRF)

Diabetes mellitus is the most common cause of CRF. Other common causes are:glomerulonephritis, chronic pyelonephritis, renal vascular disease, gout and polycystic renal disease.

Sonographically, there is an initial renal enlargement, however, with time there is a reduction in size and an increase in cortical echogenicity.(D. Buirwin,2002)

2.3.9 Renal Manifestations of Aids

Nephropathy associated with human immunodeficiency virus (HIV) infection is an important cause of AIDS morbidity. Patients present with rapid deterioration of renal function and proteinuria."1 AIDS patients are vulnerable to opportunistic infections and certain tumors (lymphoma and Kaposi’s sarcoma) as well as pyelonephritis, renal abscess and cystitis.

Sonographically the characteristic findings are enlarged kidneys with increased cortical echogenicity. “Additional findings include a globular

appearance of the kidney, decreased renal sinus fat, and heterogeneous parenchyma with echogenic striations. (G ItalNefrol. 2012**)**

2.3.10Renal infection:

Urinary tract infections (UTIs) are a common clinical problem, especially among women.

Ultrasound assessment is indicated in case of complicated UTIs, in particular in children, pregnant women and patients with chronic kidney disease. (G ItalNefrol. 2012**)**

The frequency of urinary tract infections (UTIs) is second only to that of respiratory tractinfections in the pediatric population. UTIs often are separated into infections of the lowerurinary tract that involve the bladder and urethra and those of the upper tract that involve the kidneys, renal pelvis, and ureters. Infections of the upper tract are designated pyelonephritis. (G ItalNefrol. 2012**)**.

2.3.10.1 Acute Pyelonephritis (Acute Bacterial Nephritis)

Acute pyelonephritis is infection of the renal pelvis, calyces and parenchyma.

This i/s most often (85%) caused by an ascending Escherichia coli (E. coli) infection.

The E. coli is a normal inhabitant of the bowel and because of the female urethra's close proximity to the anus, these infections are far more common in the female. The remaining 15% of acute pyelonephritis cases are caused by hematogenous seeding (of staphylococcus aurea's) from elsewhere in the body.(Kemp, 2008)

The patient presents with flank pain, fever, chills, leukocytosis, dysuria andbacteriuria. One or both kidneys may be involved.

Ultrasound is used to rule out obstructions or abscesses in patients who have not responded to antibiotics or who have progressive symptoms. Most kidneys demonstrate no abnormality however, edema may result in diffuse renal enlargement. In addition, there may be decreased parenchymal echogenicity and loss of corticomedullary differentiation. The walls of the renal pelvis or major calyces may be thickened.(Kemp, 2008)

2.3.10.2 Emphysematous Pyelonephritis (EPN)

If a gas-forming organism infects the renal parenchyma, gas may accumulate within affected portions of the renal tissue. The term emphysematous pyelonephritis' is applied to this uncommon but highly dangerous condition, which usually occurs indiabetic patients.(Kemp, 2008)

Sonographically EPN will demonstrate highly echogenic foci with distal dirty shadowing emanating from the parenchymal gas bubbles.CT is the preferred imaging choice as visualization of deeper structures is obscured with US. Also, with US, gas could be misinterpreted as arising from bowel or renal calculi.(Kemp, 2008)

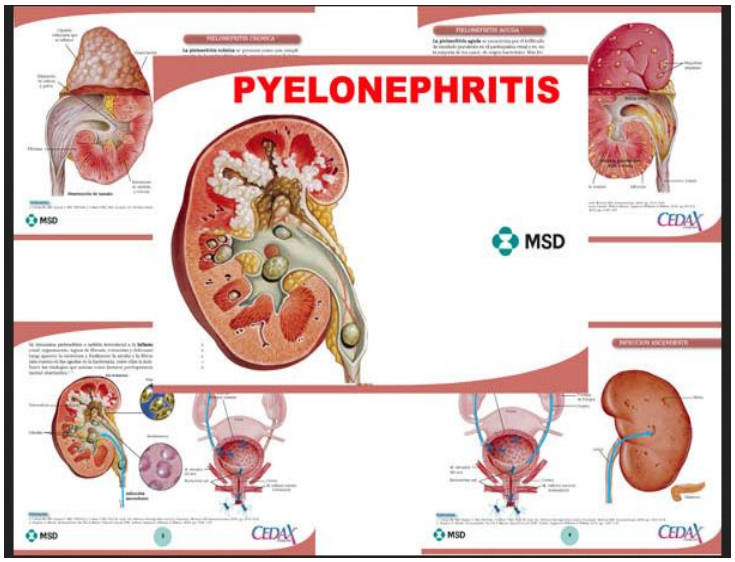

Figure. (2-7) Pyelonephritis(Kemp, 2008)

2.3.10.3 Glomerulonephritis:

Is an inflammatory process affecting primarily the glomerulus, with infiltration and proliferation of acute inflammatory cells. These are principally mononuclear cells and neutrophils in post-infectious glomerulonephritis. The inflammation is immunologically mediated with immune deposits in the glomerulus. Onset of symptoms is usually acute. Symptoms include oliguria, hypertension, hematuria, proteinuria and renal impairment.Glomerulonephritis is an important cause of renal failurethought to be caused by autoimmune damage to thekidney. While each type of glomerulonephritis beginswith a unique initiating stimulus, subsequent commoninflammatory and fibrotic events lead to a final pathwayof progressive renal damage. In this article the differentforms of inflammatory glomerulonephritis and theirdiagnosis are discussed. In a review of therapy

bothimmediate lifesaving treatment given whenglomerulonephritis causes acute renal failure and morespecific treatments designed to modify the underlyingmechanisms of renal injury are considered.(C S Vinen, D B G Oliveira.2003)

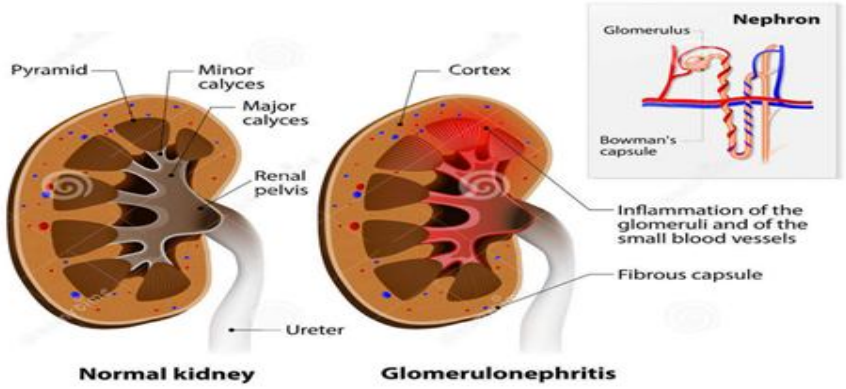

Figure. (2-8) Glomerulonephritis(Kemp, 2008)

2.4 Investigations done for kidneys:

2.4.1 Laboratory investigation:

These include:

• Urine protein—a few different tests may be used to screen for protein in the urine:

• Urine albumin—this test may be done on a 24-hour urine sample, or both urine albumin and creatinine can be measured in a random urine sample and the albumin/creatinine ratio (ACR) can be calculated. The American Diabetes Association recommends ACR as the preferred test for screening for albumin in the urine (microalbuminuria).

• Urinalysis—this is a routine test that can detect protein in the urine as well as red blood cells and white blood cells. These are not normally found in the urine and, if present, may indicate kidney disease.

• Urine total protein or urine protein to creatinine ratio (UP/CR)—detects not just albumin, but all types of proteins that may be present in the urine.

While urinalysis and urine total protein are not as sensitive as urine albumin for detecting kidney damage, these tests give fewer false signals of kidney damage.

• Estimated glomerular filtration rate (eGFR)—a blood creatinine test or possibly a cystatin C test is performed in order to calculate the eGFR. The glomerular filtration rate refers to the amount of blood that is filtered by the glomeruli per minute. As a person's kidney function declines due to damage or disease, the filtration rate decreases and waste products begin to accumulate in the blood.

Some additional tests that may be ordered to evaluate for kidney disease include:

Urea (urea nitrogen or BUN)—the level of this waste product in the blood increases as kidney filtration declines. Increased BUN levels suggest impaired kidney function, although they can also be elevated due to a condition that results in decreased blood flow to the kidneys, such as congestive heart failure, heart attack, or shock.

Creatinine clearance—this test measures creatinine levels in both a sample of blood and a sample of urine from a 24-hour urine collection. The results are used to calculate the amount of creatinine that has been cleared from the blood and passed into the urine. This calculation allows for a general

evaluation of the amount of blood that is being filtered by the kidneys in a 24-hour time period.

2.4.2 Radiological investigation:

2.4.2.1. X-ray:

An x-ray of the abdomen can show the size and position of the kidneys and urinary

Tracts include:

- Plain KUB.
- Intravenous urography (I.V.U).
- Cystogram.
- Retrograde urography.

2.4.2.2 Computer tomography (CT):

Is more expensive then ultrasound scanning and intravenous urography but has some advantage. Because CT scans can distinguish soil structures from those that contain liquids, they're most useful in evaluating the type and extent of kidney tumors or other masses distorting the normal urinary tract. A radiopaque substance can be injected intravenously to obtain more information. (Mark H, Beers M 2010).

2.4.2.3 Magnetic resonance imaging (MRI):

It can provide information about kidney structures that can't be obtained by other techniques. Addition MRI produces excellent pictures of blood vessels and structures around the kidneys, so that a wide variety of diagnoses can be made. (Mark H, Beers M 2010).

2.4.2.4 Nuclear Medicine:

Nuclear medicine studies of the kidneys involve administration of an I.V. radionuclide which is filtered through the kidneys at a specific rate and

concentration. A series of films document the effectiveness of renal perfusion and function. The disadvantages of nuclear medicine studies are they rely on function and demonstrate only gross anatomy. (Mark H, Beers M 2010).

2.4.2.5 Ultrasound:

Ultrasound scanning uses sound waves to produce image of anatomic structures. The technique is simple, painless, and safe. Ultrasound scanning is an excellent way to estimate kidney size and to diagnose a number of kidney abnormalities. (Mark H, Beers M 2010).

2.5 Scanning technique:

The examination begins with the patient in the supine position. Scans are performed in the sagittal and transverse planes from the anterior approach using the liver and spleen as acoustic windows. Various maneuvers may enhance demonstration of the kidneys: left lateral decubitus or lateral oblique positions for the right kidney and right lateral decubitus or lateral oblique positions for the left kidney. Coronal longitudinal and transverse scans may also be obtained and are recommended for evaluating the renal pelvis and proximal Ureter on hydronephrotic patients.(Tempkin, (1999).

The highest frequency transducer permitting adequate penetration is used. This is usually in the 3 to 5 MHz range. A phased array sector probe with its small footprint permits subcostal and intercostal scanning.(Tempkin, (1999).

Figure. (2-9) Pt position for Lt kidney

Figure. (2-10) Pt position for Rt kidney

2.7 NormalSonographic Appearances of Adult Kidneys

The kidney is an ellipsoid structure when demonstrated in its long axis. The capsule is an echogenic white boundary separating the kidney from adjacent structures anteriorly and the musculature posteriorly.(Tempkin, (1999).

Per renal fat is highly echogenic. The renal cortex is homogeneous, fine textured and poorly echogenic. The cortex is equal to, or less echogenic than the normal liver.(Tempkin, (1999).

The renal columns (septal cortex or columns of Bertin) are the projections of cortex that extend between the pyramids. The columns are son graphically identical to the peripheral cortex.(Tempkin, (1999).

The medulla consists of pyramids which are anechoic structures with their bases adjacent to the renal cortex and their apices directed towards the renal sinus.(Tempkin, (1999).

The renal sinus is the most echogenic portion of the adult kidney. This echogenic area is called the central echo complex. In the nonhydrated state the renal pelvis is collapsed.(Tempkin, (1999).

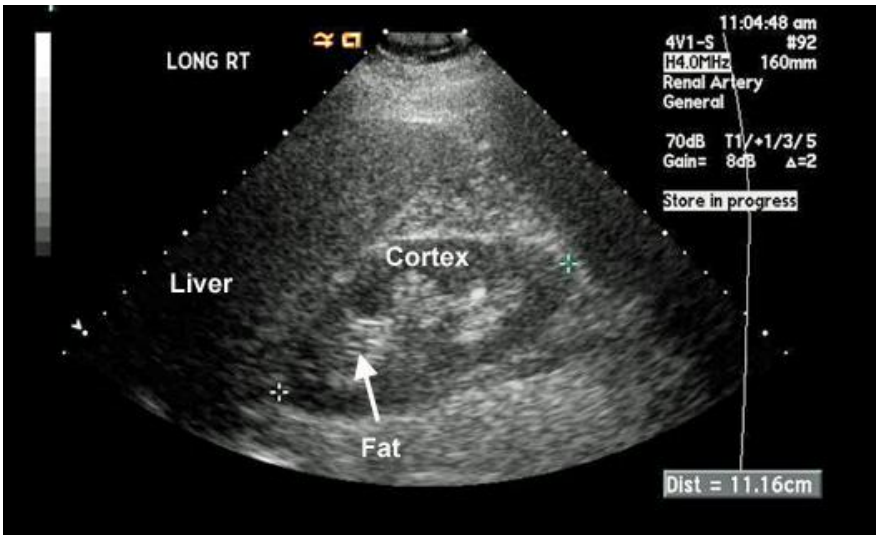

Figure. (2-11) Sonographic Appearances of normal kidney

The sizeof the kidneys is affected by age, sex (greater in men than in women), andbody size; furthermore, the left kidney is slightly larger than the right in mostindividuals. (D. Buirwin, 2002)

The normal renal length in females ranges from 9.5 to 12.1 cm and in males from 10.1to 12.6 cm.2 Therefore, the normal adult kidney should measure 9-13 cm in length,12.5 to 3.5 cm3,4 in thickness and 4 to 5 cm in width3,4.These are good averagemeasurements for exam purposes. (D. Buirwin, 2002)

Body habitus and age should be considered since a single measurement couldmisrepresent the patient's condition. A 10 cm long kidney is a normal renal length; however, it is likely to be abnormal in a 20 year old male who is 6 feet tall and weighs200 pounds.Parenchymal thickness is 11-18 mm in the male and 11-16 mm in thefemale. (D. Buirwin, 2002)

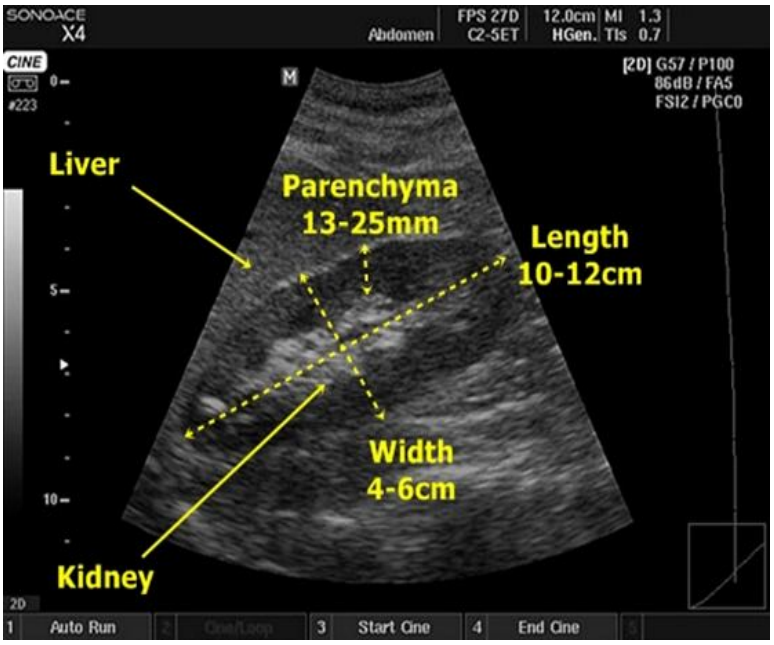

Figure. (2-12) Normal Renal Measurements

Renal volume is a more sensitive indicator of size. In certain clinical settings such asrenal transplant recipients, it may be necessary to obtain a renal volume on thekidney. The formula is:

Measurements of median renal volume in adults range from 134 to 150 ml. Again with men larger than women and the left kidney larger than the right. There is correlation between the renal volume and weight of the patient. (D. Buirwin, 2002)

Renal Pelvis Size - If the patient is non-hydrated, the renal pelvis is collapsed and therefore not demonstrated on the scan. However, the renal pelvis is influenced by many factors (bladder distention, diuretic drug effects) and in an estimated 5% ofNon-hydratedpatients, there will be an

anechoic separation of the central echo complex indicative of the renal pelvis. (D. Buirwin, 2002)

Distention of the renal pelvis is seen in 50% of no hydrated patients and in 90% of hydrated patients examined with a full bladder.

The normal renal pelvis in the hydrated adult patient is between 2 and 14 mm. (D. Buirwin, 2002)

PEDIATRIC

The most commonly used measurement standard is renal length compared with chronological age.

Normal renal length of the pediatric kidney may be determined using the following guide: (D. Buirwin, 2002)

Over one year - renal length in cm. = 6.79 + (0.22 x age in years)

Less than one year - renal length in cm. = 4.98 + (0.155 x age in months)

"Asymmetry in renal lengths exceeding 5 mm in infants and 10 mm in older children should raise the suspicion of an underlying problem even if both kidneys are within the normal range. (D. Buirwin, 2002)

2.8 Texture Analysis

Texture is an important characteristic of images and refers to the appearance of the image. Image texture is a function of the spatial variation of pixel intensities in an image(Conners RWet.al 1980) (Kjer L et.al 1995) Image texture analysis can provide quantitative information in the form of texture features that is not visible to human vision(Haralick RM et.al 1973)Texture features are mathematical parameters computed from the distribution of pixels, which characterize the texture type in the image. The

most common method of computing the image texture is to use a statistical based method that analyzes the properties of individual pixel intensities and their spatial distribution within the image (Haralick1979) . Statistical based texture analyses are commonly classified as first-order and second order textures, based on the number of pixels defining the local features. First-order textures estimate properties of individual pixel values, ignoring the spatial interaction between the neighboring image pixels, whereas second-order textures estimate properties of two or more pixel values occurring at specific locations relative to each other.

2.8.1 First-Order Textures

Textures based on first order statistics are features that can be computed from the gray level histogram. The histogram of an image is the count of the number of pixels in the image that possess a given grey-level value.

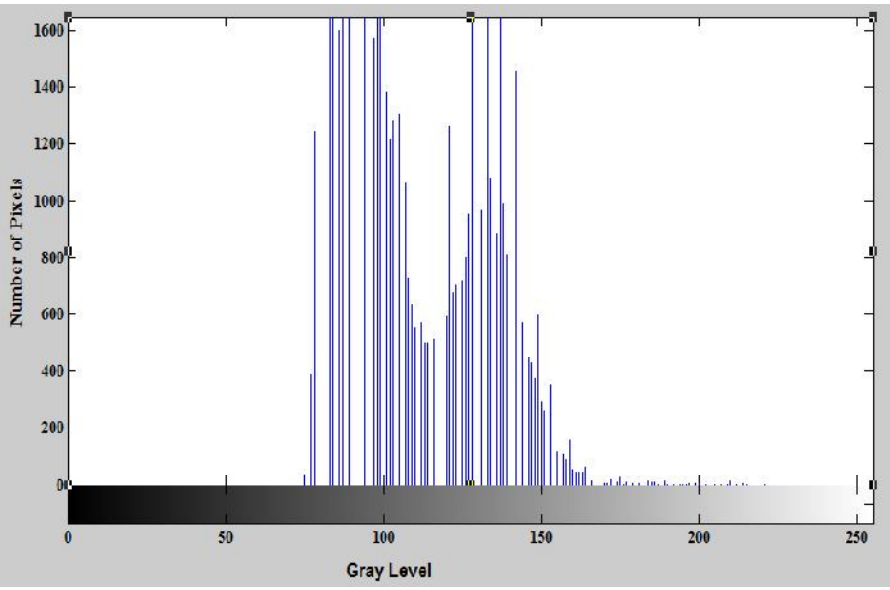

Figure(2-13) Gray-level histogram

(1) Mean of the histogram is the mean of the gray-levels in an image.

$$\bar{x} = \frac{1}{n} \sum_{i=1}^{n} x_i \qquad [1.9]$$

x = gray levels

n = number of gray-levels

n = (2) Standard deviation is a measure of how far from the mean the gray values in the image are distributed.

$$s = \sqrt{\frac{1}{n} \sum_{i=1}^{n} (x_i - \bar{x})^2} \qquad [1.10]$$

(3) Skewness of the histogram refers to the asymmetry of the distribution of the gray values. A distribution is symmetric if the right side of the distribution is similar to the left side of the distribution. If the distribution is symmetric, then the skewness value is zero. A distribution with an asymmetric tail extending out to the right is referred to as positively skewed, while a distribution with an asymmetric tail extending out to the left is referred to as negatively skewed. The skewness of a distribution is defined as:

$$sk = \frac{\frac{1}{n} \sum_{i=1}^{n} (x_i - \bar{x})^3}{\left[\sqrt{\frac{1}{n} \sum_{i=1}^{n} (x_i - \bar{x})^2} \right]^3} \qquad [1.11]$$

(4)

Kurtosis is a measure of how flat or peaked the top of a symmetric distribution is when compared to a normal distribution. If the grey level distribution is similar to the 34 normal distribution, the kurtosis value is 3. Flat-topped distributions are referred to as platykurtic and have a kurtosis value of less than 3, while less flat-topped distributions are referred to as leptokurtic and have a kurtosis value greater than 3. The kurtosis of a distribution is defined as:

$$k = \frac{\frac{1}{n}\sum_{i=1}^{n}(x_i - \bar{x})^4}{\left[\sqrt{\frac{1}{n}\sum_{i=1}^{n}(x_i - \bar{x})^2}\right]^4} \qquad [1.12]$$

The limitation of the histogram-based measurements is that they carry no information

regarding the relative spatial position of pixels with one another. The spatial relationship of the pixels can be incorporated by taking in to account the distribution of intensities as well as the position of pixels with equal or nearly equal intensity values. This can be achieved by constructing a gray level co-occurrence matrix as explained in the next section.

2.8.2 Second-Order Textures

Textures based on second-order statistics are features that can be computed from the gray level co-occurrence matrix (GLCM). The GLCM is a two-dimensional histogram of graylevels for a pair of pixels separated by a fixed distance (d) at a fixed angle (θ). (Haralick RM1979), It is an estimate of the joint probability G(i, j) of the intensity values of two pixels (i and j), at a certain pixel distance apart along a given direction (i.e., the probability that i and j have the same intensity). This joint probability takes the form of a square matrix with row and column dimensions equal to the number of discrete gray levels (intensities) in the image. If an intensity image contained no texture (intensity variations) the resulting GLCM 35 would be completely diagonal. As the image texture increases (i.e. as the local pixel intensity variations increase), the off-diagonal values in the GLCM become larger. GLCMs are usually computed with neighboring pixels defined in angular directions 0^o, 45^o, 90^o and 135o. Figure 2.2 shows an example to construct a GLCM. Consider a 4x4 image (Figure 1.17a) with 4 gray-levels

from 0 to 3 (Figure 1.17b). A generalized GLCM is shown in Figure 1.17c where (i, j) stands for the number of times gray-level i and j satisfy the condition stated by the offset distance vector d and angle θ. The resulting four GLCMs for d = [0 1] and [0 -1] and θ = 0o, 45o, 90o, 135o are shown in Figure 1.17d-g.

0	0	1	1
0	0	1	1
0	2	2	2
2	2	3	3

Figure. (2-14)Smapmlepilmeiamgea. g e. Gray-levels in the **Sample**

(i, j)	0	1	2	3
0	(0,0)	(0, 1)	(0, 2)	(0, 3)
1	(1,0)	(1, 1)	(1, 2)	(1, 3)
2	(2,0)	(2, 1)	(2, 2)	(2, 3)
3	(3,0)	(3, 1)	(3, 2)	(3, 3)

Figure 1.17c: general form of a GLCM

4	2	1	0
2	4	0	0
1	0	6	1
0	0	1	2

Figure 1.17d: GLCM for θ = 0°

4	1	0	0
1	2	2	0
0	2	4	1
0	0	1	0

Figure 1.17e: GLCM for θ = 45°

6	0	2	0	2	1	3	0
0	4	2	0	1	2	1	0
2	2	2	2	3	1	0	2
0	0	2	0	0	0	2	0

Figure 1.17d: GLCM for θ = 90° **Figure 1.17e: GLCM for θ = 135°**

GLCMs as seen above are symmetric matrices. Hence either upper or lower triangle is used for calculation of the second-order features. Each e probability of co-occurrence of the pixel gray-levels. The second-order texture features can then be calculated using the formulas shown below. Each of the five GLCM-based second-order texture features that are used in this thesis are described below:

(1) Entropy is the measure of randomness of the GLCM. It describes the amount of chaos or disorder within the elements of the GLCM. Entropy is higher when the image isnon-uniform.

$$Entropy = -\sum_{i,j} G(i,j)\, log_2 G(i,j) \qquad [1.13]$$

G(i, j) = probability of co- occurrence of the pixel gray-levels

(2) Homogeneity measures the closeness of the distribution of elements in the GLCM to the GLCM diagonal. It is also known as inverse difference moment. It is sensitive to the near diagonal elements of the GLCM. It is higher for a diagonal GLCM.

$$Homogeneity = \sum_{i,j} \frac{1}{1+|i-j|} G(i,j) \qquad [1.14]$$

(3) Inertia measures the intensity or gray-level variation between the reference pixel and its neighbor over the whole image. It describes the local variations in the GLCM. It is inaversely correlated to homogeneity and will be lower for a diagonal GLCM.

$$Inertia = \sum_{i,j}(i-j)^2 G(i,j) \quad [1.15]$$

(4)

Correlation measures how correlated a reference pixel is to its neighbor over the whole image. It describes the joint probability occurrence of the specified pixel pairs.

Correlation is 1 or -1 for a perfectly positively or negatively correlated image.

$$Correlation = \sum_{i,j} \frac{(i-\mu)(j-\mu)G(i,j)}{\sigma^2} \quad [1.16]$$

μ and σ are the mean and standard deviation.

(5) Energy describes the uniformity of the image. It measures the sum of squared

elements of the GLCM. It is also known as angular second moment feature. Energy is high if the image is homogenous.

$$Energy = \sum_{i,j} G(i,j)^2 \quad [1.17]$$

2.8.3 Texture Analysis of Medical Images

US images hold a large amount of texture information that may be relevant for clinical diagnosis. Due to its inherent resolution limitation, US images are not capable of providing microscopic tissue information that can be evaluated visually. However, histological changes present in various diseases may generate textural changes in the US image that can be quantified through texture analysis.

2-9previous study:

Image texture analysis has been used in a range of US studies for classifying tissues in renal infections.

Texture analysis for computer-aided diagnosis (CAD) in medical images has been studied in many disciplines including the diagnosis of breast cancer in mammograms (Sahiner .S et al, 1998 - Zhang. M et al, 1996), lung nodules in chest radiographs [6-8], osteoporosis in bone x-ray images (Lan. L et al, 2007-. Wilkie.J.et al, 2004), and abnormalities in kidney and liver (Lee G.N. et al, 2006-. Kim. D et al, 2004). Analysis is typically based on regions-of-interest (ROIs). In this essence there are a number of different definitions of texture, when applied to image data. All definitions have in common the fact that they describe texture as an attribute of an image window. Texture is one of the important characteristics used in characterizing objects or regions of interest; (M Haralick et al, 1979-1973) developed a set of statistical features for classifying pictorial images. Chevaillier and Ponvianne proposed a semi-automated method to segment internal structures from a DCE-MRI registered sequence. They segmented cortex, medulla, and pelvis regions using the k-means partitioning algorithm. Pixels were classified according to their intensity (Chevaillier .B et al, 2008). Marcuzzo and Masiero segmented kidneys using the Expectation Maximization (EM) algorithm. They proposed 5 different classification methods to distinguish normal kidneys from rejected kidneys. They used symmetry of two kidney images, shape, relative position, boundaries, and radiopharmaceutical information in DRE-MRI. They used 20 training kidney subjects to build reference information for these classification methods. For shape information they averaged 20 left and 20 right kidneys and determined a reference mean shape for a normal kidney (Marcuzzo et al. 2007). Koh and Shen suggested a segmentation procedure based on a generated rectangular mask and edge information to overcome the problem that no prior information about location or appearance exists. They also used threshold values in segmentation step. However, organs in DRE-MRI have similar gray level information. Also cortex, medulla, and

pelvis regions of kidneys have similar gray level value in some scans. Therefore, segmentation based on threshold will not work to segment cortex and medulla regions in their case (Koh. M. et al, 2006).Xie and Jiang proposed kidney segmentation from ultrasound images based on texture and shape priors. Texture features were obtained by applying Gabor filters on images through a two-sided convolution strategy (Xie. J. et al, 2005).

Wan (2012)proposed an approach of feature extraction of kidney ultrasound images based on five intensity histogram features and nineteen gray level co-occurrence matrix (GLCM) features. Kidney ultrasound images were divided into four different groups; normal (NR), bacterial infection (BI), cystic disease (CD) and kidney stones (KS). Before feature extraction, the images were initially preprocessed for preserving pixels of interest prior to feature extraction. Preprocessing techniques including region of interest cropping, contour detection, image rotation and background removal, have been applied. Test result shows that kurtosis, mean, skewness, cluster shades and cluster prominence dominates over other parameters. After normalization, KS group has highest value of kurtosis (1.000) and lowest value of cluster shades (0.238) and mean (0.649) while NR group has highest value of mean (1.000), skewness (1.000), cluster shades (1.000) and cluster prominence (1.000). CD group has the lowest value of skewness (0.625) and BI has the lowest value of kurtosis (0.542). This shows that these features can be used to classify kidney ultrasound images into different groups for creating database of kidney ultrasound images with different pathologies.

FontanillaT et al. (2012) described 48 patients in detail the CEUS findings in acute pyelonephritis, and to determine if abscess and focal pyelonephritis may be distinguished. Very characteristic morphologic and temporal patterns of enhancement are described. These allow differentiation of focal

pyelonephritis from renal abscess, and detection of tiny supportive foci within focal pyelonephritis. The detection of abscesses is important because follow-up in 25 patients revealed a longer clinical course. Typical pyelonephritis CEUS features permit distinction from other renal lesions. As a whole, CEUS is an excellent tool in the work-up of complicated acute pyelonephritis, so it may be considered as the imaging technique of choice in the evaluation and follow-up of these patients who frequently are very young, so as to minimize radiation exposure.

.

A. Hassan et al(2014) intended to measure the ultrasound normative values of renal length and parenchymal thickness in adult Sudanese population in order to establish their reference value for Sudanese population while no recorded reference value in literature for them. Ultrasonographic kidney measurements were performed on 77 adult patients without known kidney lesions. Measurements included length and parenchymal thickness. The effect of age, gender, site (left and right side) and height was statistically analyzed. All normal patient was included in this study while any renal disease were excluded. This study was include (35) males and (42) females. The mean renal lengths were (10.15± 0.78) and (10.33± 0.80) cm for the right and left kidney respectively. The mean parenchymal thicknesses were (1.4714± 0.33cm) for the right kidney and (1.7169± 0.36cm) for the left kidney. They found there were correlated with age, gender, site, and height which showed that there is no significant difference between right and left renal length, but there was significant difference between right and left parenchymal thicknesses. The significant effect of age was found only in left renal length. The significant effect of gender was noted only in the right parenchymal thicknesses. No significant difference among height groups for renal length, but there was significant difference in right parenchymal

thickness. The study concluded that normal value of left renal length was affected with age and normal parenchymal thickness was affected with site (left or right). The right parenchymal thickness was affected with gender and height. Establishment of normal renal values of renal length and parenchymal thickness in Sudanese population will help us in evaluation of patients with chronic renal disease.

Brandt et al. (1982) assessed normal renal dimensions using Ultrasound. Their study confirms that the accuracy and reliability of sonographic assessment of renal dimensions when meticulous scanning techniques are employed. Sonographic renal dimensions are smaller than those obtained by radiography, since there is neither the geometric magnification nor the change in size related to an osmotic dieresis from iodinated contrast material. Sonographically, with patients in the prone position, the mean right renal length was 10.74 cm (± 1.35 SD) and the mean left renal length was 11.10 cm (± 1.15 SD). A prospective sample demonstrated the mean depth (ventral-dorsal dimension) to be approximately 4.5 cm when the transducer was angulated for the lie of the kidney.

Shin et al. (2009) measured the Kidney Volume with Multi-Detector Computed Tomography Scanning in Young Korean to estimate the normal kidney volume of healthy young Korean men and evaluated its predictability of renal function and relationship with body indexes. Their study included 113 patient Images were obtained prior to and after the administration of 150 mL of iodinated contrast media during the parenchymal phases of enhancement. The kidney size was measured using GE Advantage Windows Workstation, and kidney length was measured using coronal sections. Maximum kidney length was calculated from all coronal sections. The kidney volume was measured from contiguous slices. In coronal section images with parenchymal enhancement, the region of

interest was drawn around the kidney, and the slices were reconstructed at 1-mm intervals to obtain a 3-D volume-rendered image of the kidney. The volume was calculated by multiplying the sum of areas from each slice by the reconstruction interval at the workstation. Their results showed that the mean kidney volume was 205.15 cm2 (138.53-359.6 cm2). The left kidney was significantly ($p < 0.05$) larger than the right kidney, and they were highly correlated (correlation coefficient: $r = 0.874$, $p < 0.05$). The mean kidney length was 108.02 cm (9.09-12.49 cm). The left kidney was also significantly ($p < 0.05$) longer than the right kidney. The kidney length and kidney volume were highly correlated reciprocally ($r = 0.671$, $p < 0.05$)

Segmentation of the kidney into classes using texture is a challenging task in respect to the classifier and the type of texture. Therefore there are a number of different definitions of texture, when applied to image data. All Definitions have in common the fact that they describe texture as an attribute of an image window. These attributes can represent spatially deterministic aspects of the Grey level, including its stochastic color distribution properties (wagner1999).Goal et al. (1984) defined texture as structure composed of a large number of more or Less ordered similar patterns without any one of these drawing special attention. A Pattern like a checkerboard is said to have a deterministic texture, having a regular or

Nonrandom texture. Conversely the structure might resemble noise as on a television Monitor screen, and such a texture is said to be stochastic or statistically based on random Fluctuations. The two major characteristics of textures are its coarseness and Directionality, thus the two major texture analysis approaches are statistical and Structural.

Texture is one of the important characteristics used in characterizing objects or Regions of interest. Heraldic et al. (1973) and hadalick (1979) developed

a set of Statistical features for classifying pictorial images. The statistical features are based on A matrix derived from the spatial distribution of grey level values in the pixels of the Image. This matrix is known as the spatial grey level dependence (SGLD) matrix. The Sgld matrices describe how often pairs of pixels, which are separated by a certain Distance and lie along a certain direction, occur in a digital image with some texture .Generally sgld matrices are not used directly, but statistical quantities based on They are computed to describe the characteristics of the textures. Texture features, Also referred to as haralick features can be computed from the sgld matrix. Some Of these measures are related to specific textural characteristic of the image such as Homogeneity, contrast, greys level linear dependence, or complexity of the image .Even though these texture features contain information about the texture characteristic Of the image it is hard to identify which specific texture is represented by each of Those features. These textural measures include entropy, energy, inverse Difference moments, sum entropy, correlation, Difference average, sum variance, information measure of Correlation (1) and variance and are detailed in Section 4.

A number of algorithms can be used to select the optimum subset of features, to avoid Redundancy and co-linearity between the features (Tourassi, 2001) used mutual information as a criterion for feature selection for a Non-linear classifier. Mutual information selection criteria need a large data set and Also depend upon the number of histogram bins that are determined empirically. This Is thus a limited method of feature selection.

Walker et al. (2003) used genetic algorithms for texture feature selection. The basic Approach was to create a combination of randomly selected texture features. Each Combination was considered a possible solution. The main advantage of a genetic A number of algorithms can be used to select

the optimum subset of features, to avoid Redundancy and co-linearity between the features.

Algorithm is its ability to investigate many possible solutions simultaneously. Although successful, genetic algorithms are computationally very demanding, particularly as the number of available features increases. Texture features have been used in medical imaging for many purposes, for example To classify and assess renal tissues in MR images.

Chapter Three

3. Materials and Methods

3.1 Ultrasound machine:

Renal ultrasound examination was performed withMindary DC-7and My lab 60ultrasound machines with 3.5-5 MHz probe is typically used to scan the kidney.

3.2 Design of the study:

This study is analytic study of a case control type deals with Sonographic pattern of renal infections.

3.3 Population of the study:

The population of this study consisted of two groups of patient, those with normal kidneys free from any pathology as control group, group two patient diagnosed as having renal infections (glomerulonephritis and pyelonephritis). The study includes both genders with their age ranged from 11 years to 80years old. Laboratory test were included in the study

3.4 Sample size and type:

This study consisted of 234 patients having ultrasound examination, referred to urology department for investigation. Patients were selected conveniently.

3.5 Place and duration of the study:

This study was carried out in the period from January2014to Augast 2016 in Khartoum hospital ,Madani hospital , Elmanagil hospital and Elkramit family health center

3-6 Methods of data collection

Technique

The kidneys should be assessed in the transverse and coronal plane. Optimal patient positioning varies; supine and lateral decubitus positions often suffice, although oblique and occasionally prone positioning may be necessary (e.g., obese patients). Usually, a combination of subcostal and intercostal approaches is required to evaluate the kidneys fully; the upper pole of the left kidney may be particularly difficult to image without a combination of approaches.

3-7 Methods of data analysis:

After that US imageswere stored in computer disk were viewed by the Radiant, Ant DICOM Digital imaging and communication on medical in computer to selected the cronal images that suit the criteria of research population then uploaded into the computer based software Interactive Data Language (IDL) where the DICOM image converted to TIFF format to suit IDL platform. Then the image were read by IDL in TIFF format and textural features that represent the first order were extracted from the medulla and pelvic calycle system from the three groups, these features include mean, standard deviation, signal to noise ratio, energy and entropy using a window of 3×3 pixel from all data set using medulla and pelvic calycle system as Region of Interest (ROI) through an algorithm written in Interactive Data Language (IDL) software. The extracted features were classified using stepwise linear discriminant analysis using medulla and pelvic calycle system as separate data set where each include the previous three groups; in order to find the most discriminant textural feature in each set as well as the classification accuracy and sensitivity concerning the characteristics of each set.

.

3-7 Ethical approval

The ethical approval was granted from the hospital and the radiology departments; which include commitment of no disclose any information concerning the patient identification as well as consent from the patients.

Chapter Four

Results

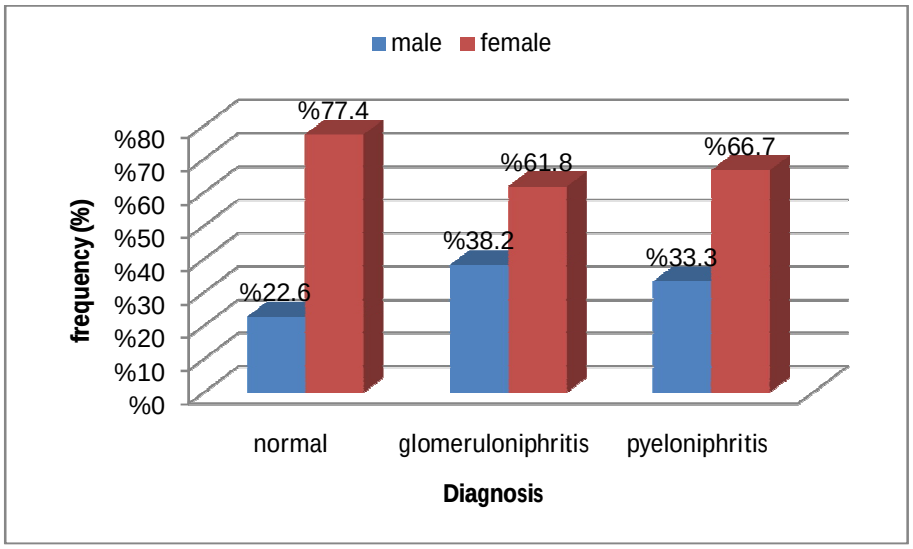

Figure 4-1: a bar graph illustrate the % frequency distribution of diagnosis according to their gender

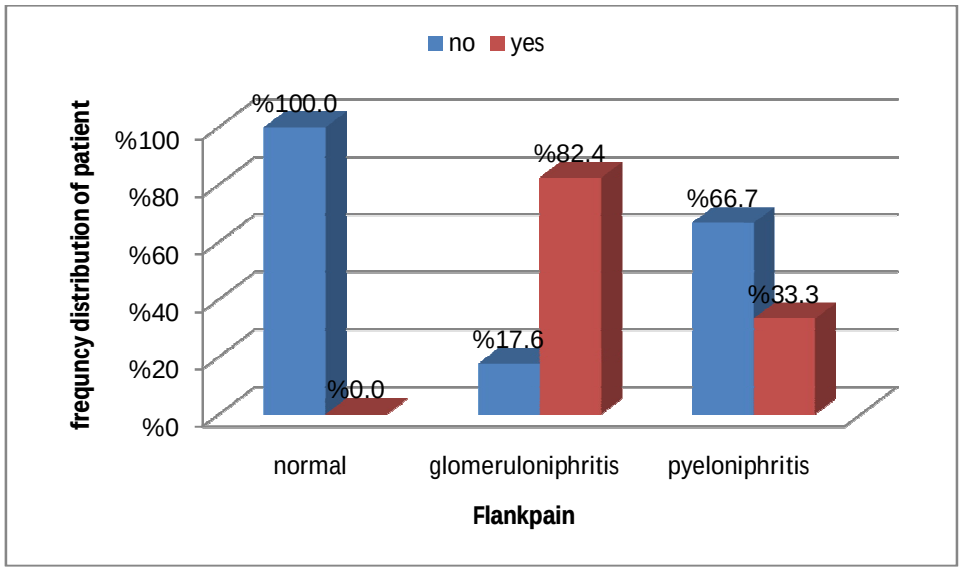

Figure 4-2.: a bar graph display the frequency distribution of flank pain

Table 4-1.the mean ± Standard deviation of the laboratory and Sonographic measured variable included in the study including the t-test values and the probability level (significant < 0.05)

Variables	Mean	Std. Deviation	t	Sig. (2-

					tailed)
RBC	Normal	0.4	0.9	8.96	**0.000**
	Abnormal	24.5	19.4		
WBC	Normal	6230.8	1113.5	16.52	**0.000**
	Abnormal	13414.9	2908.6		
Protein	Normal	0.0	0.0	12.97	**0.000**
	Abnormal	1.7	0.9		
Urea	Normal	21.8	5.4	1.29	0.200
	Abnormal	24.0	10.6		
Pus cells	Normal	1.3	1.1	15.43	**0.000**
	Abnormal	50.1	22.8		
Keratin	Normal	0.9	0.2	7.109	**0.000**
	Abnormal	0.6	0.3		
Rt Kidney length	Normal	8.3	0.9	6.162	**0.000**
	Abnormal	9.6	1.3		
Rt kidney width	Normal	4.1	0.7	0.754	0.453
	Abnormal	4.0	0.6		
Rt kidney thickness	Normal	2.9	0.3	0.071	0.944
	Abnormal	2.9	0.4		
Rt Kidney size	Normal	98.7	30.0	2.033	0.045
	Abnormal	111.6	33.1		
Rt Cortical thickness	Normal	1.9	0.4	1.786	**0.001**
	Abnormal	1.6	0.2		
Lt Kidney length	Normal	8.6	0.9	4.714	**0.000**
	Abnormal	9.6	1.1		
Lt kidney width	Normal	4.6	0.7	1.185	0.239
	Abnormal	5.4	4.9		
Lt Kidney thickness	Normal	2.9	0.4	1.698	0.093
	Abnormal	2.8	0.3		
Lt Kidney size	Normal	115.1	31.0	1.544	0.129
	Abnormal	142.5	123.6		
Lt Cortical thickness	Normal	1.9	0.4	1.544	**0.002**
	Abnormal	1.7	0.3		

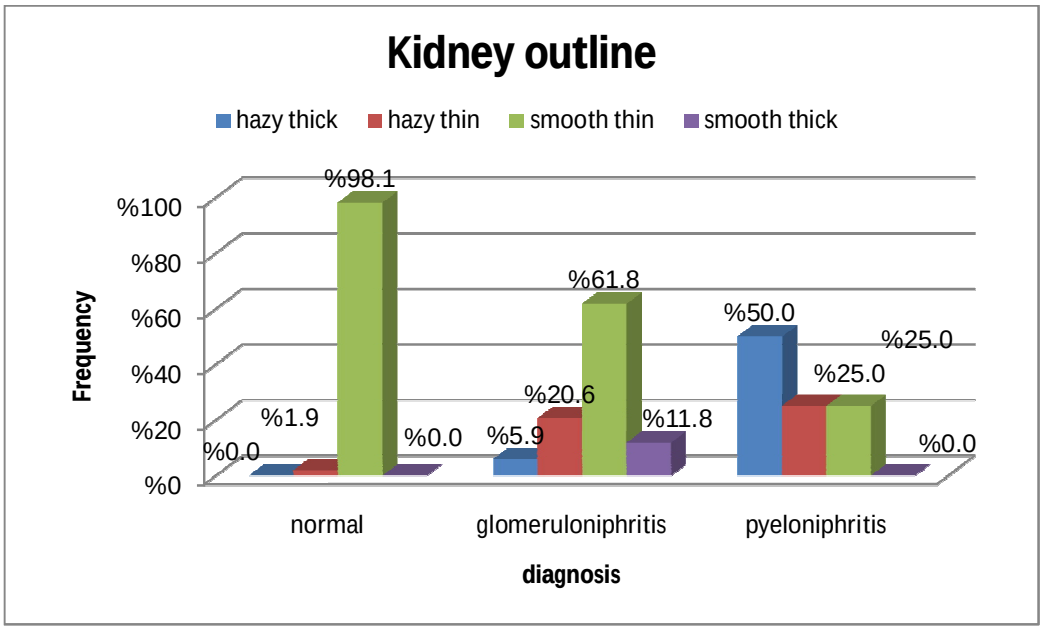

Figure 4-3.Percentage distribution of ultrasound appearances of kidney outline for normal kidneys and infected one (glomerulonephritis and pyelonephritis).

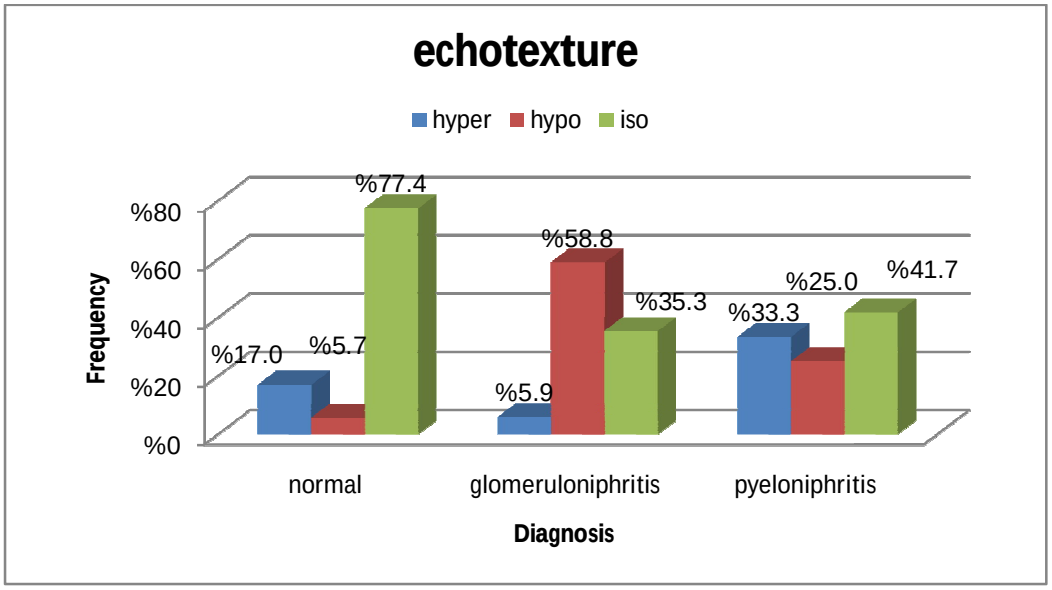

Figure4-4.Percentage distribution echo texture of normal kidneys and the affected kidneys by glomerulonephritis and pyelonephritis

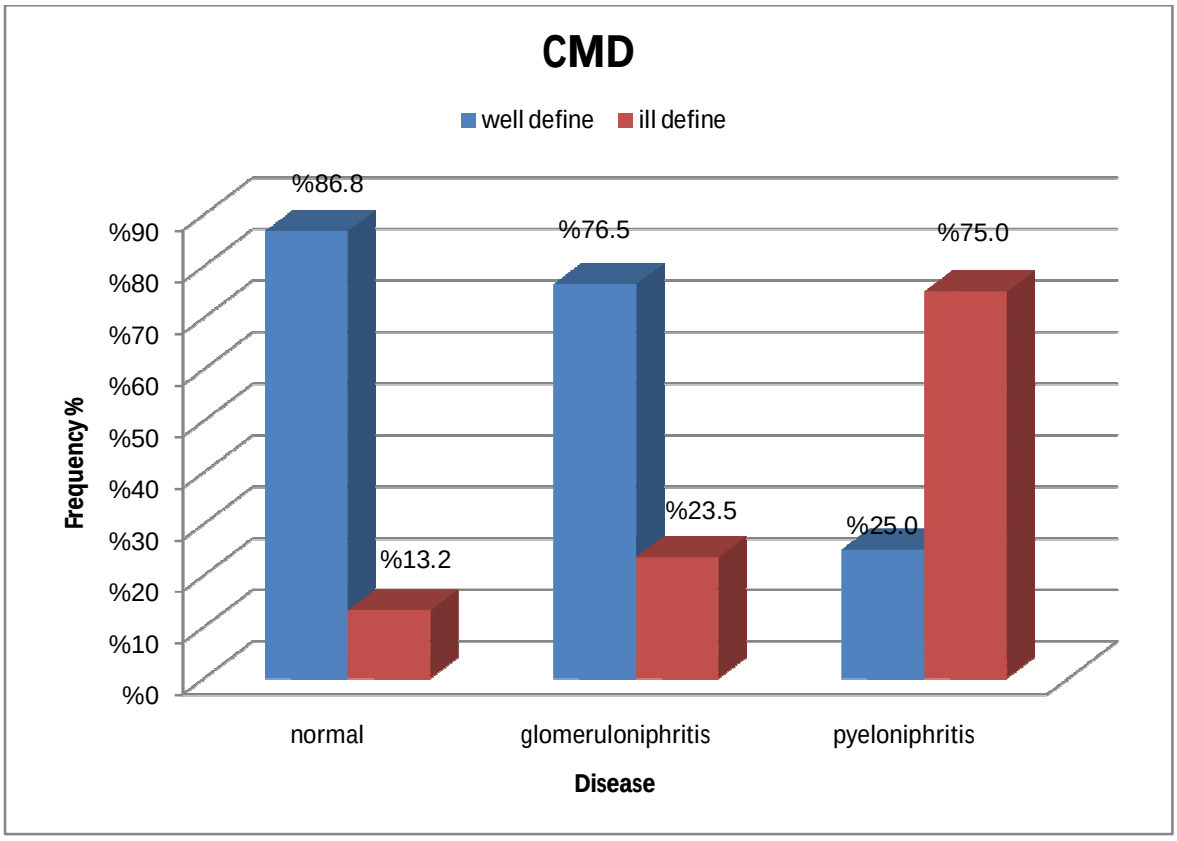

Figure 4-5. Percentage distribution of ultrasonography appearance of corticomedullary differential of normal kidneys and the affected kidneys by glomerulonephritis and pyelonephritis

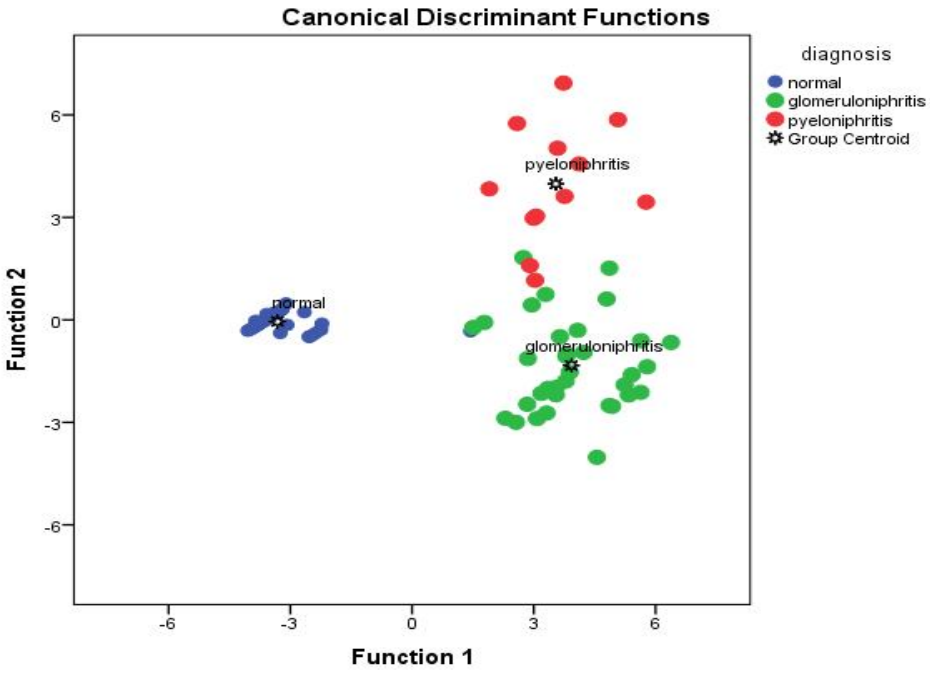

Figure 4-6. Scatter plot depicted the classification of kidney status as normal, glomerulonephritis and pyelonephritis using discriminant analysis and characteristics extracted from the ultrasound appearance features (kidney length, cortical thickness and CMD) as well as laboratory test RBC and WBC includingthe presence of flank pain.

Table 4-2. Classification score table related the accuracy of the predicted groups to the original group using the ultrasonography characteristics and laboratory tests result

	Predicted Group Membership			
Original group	Diagnosis	Normal	Glomerulonephritis	Pyelonephritis
	Normal	98.1%	1.9%	0%
	Glomerulonephritis	0%	94.1%	5.9%
	Pyelonephritis	0%	8.3%	91.7%

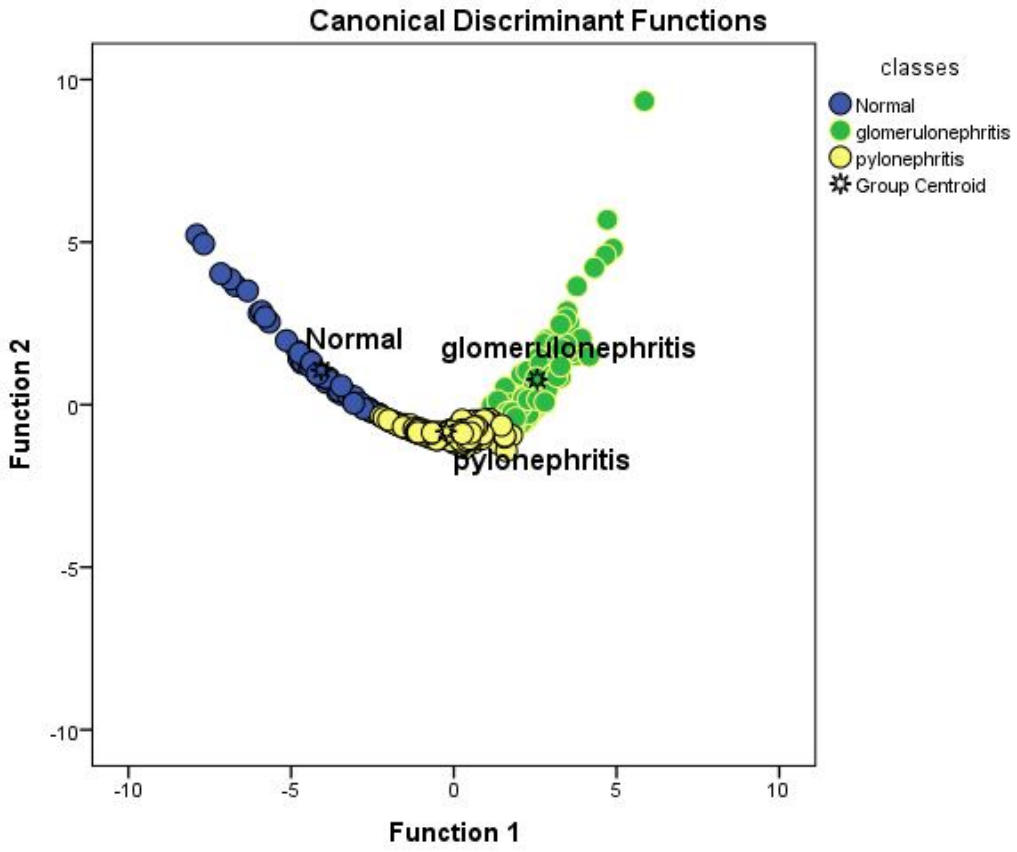

Figure 4-7. Scatter plot show the classification of textural feature that extracted from medulla of the kidney classes (normal, glomerulonephritis and pyelonephritis) using linear discriminant analysis

Table 4-3 a confusion matrix shows the classification accuracy of the selected textural features for the medulla in the normal kidney and normal, glomerulonephritis and pyelonephritis kidneys

Classes		Predicted Group Membership			Total
		Normal kidney	Glomerulonephritis	Pyelonephritis	
Original groups	Normal kidney	94.9%	0.0%	5.1%	100.0%
	Glomerulonephritis	0.0	97.3%	2.7%	100.0%
	pyelonephritis	0.0	0.5%	99.5%	100.0%

98.0% of original grouped cases correctly classified.

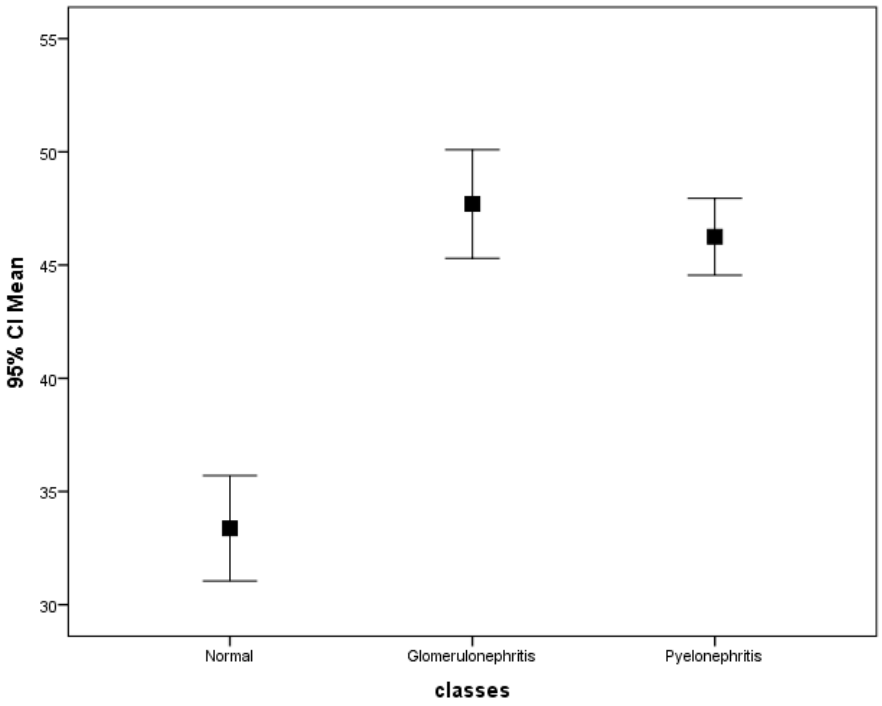

(A)

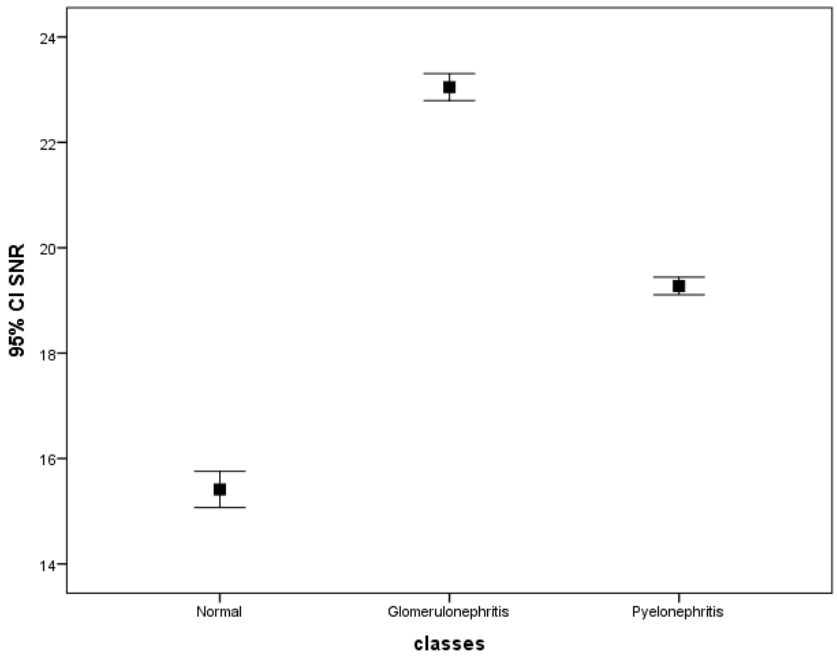

(B)

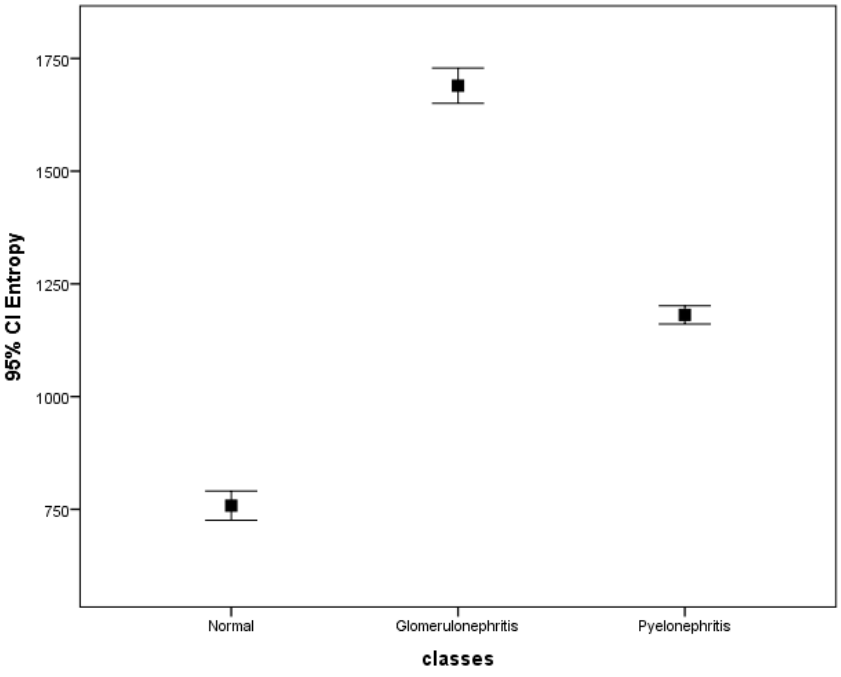

(C)

Figure 4-8. An error bar graphs of textural features (A) mean, (B) signal to noise ratio and (C) entropy for the different classes of the normal, glomerulonephritis and pyelonephritis of the medulla of the kidneys.

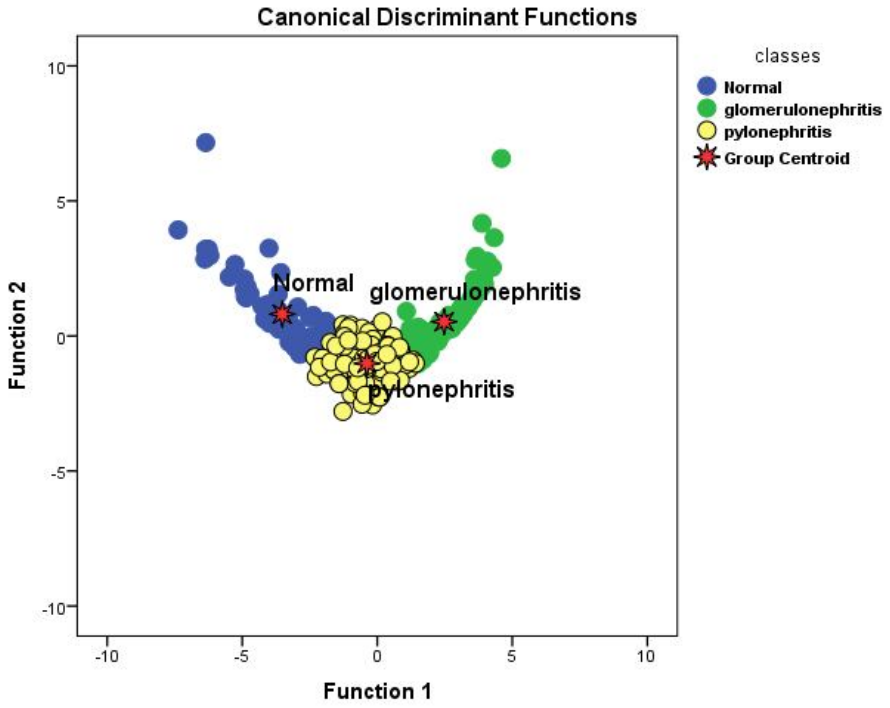

Figure 4-9. Scatter plot show the classification of textural feature of the kidneypelvic calycleclasses (normal, glomerulonephritis and pyelonephritis) using linear discriminant analysis

Table 4-4 a confusion matrix shows the classification accuracy of the selected textural features for the pelvic calycle in the normal kidney and normal, glomerulonephritis and pyelonephritis kidneys

Classes		Predicted Group Membership			Total
		Normal kidney	glomerulonephritis	pyelonephritis	
Original groups	Normal kidney	92.6%	0.0%	7.4%	100.0%
	glomerulonephritis	0.0	93.4%	6.6%	100.0%
	pyelonephritis	0.0	0.0%	100.0%	100.0%

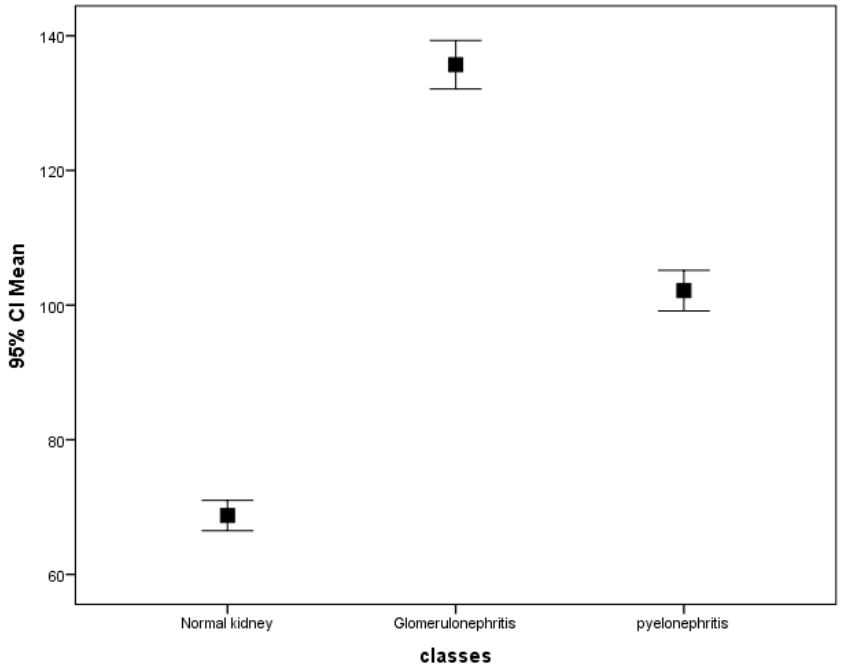
140
120
100
80
60
95% CI Mean
Normal kidney
Glomerulonephritis
pyelonephritis
classes

(A)

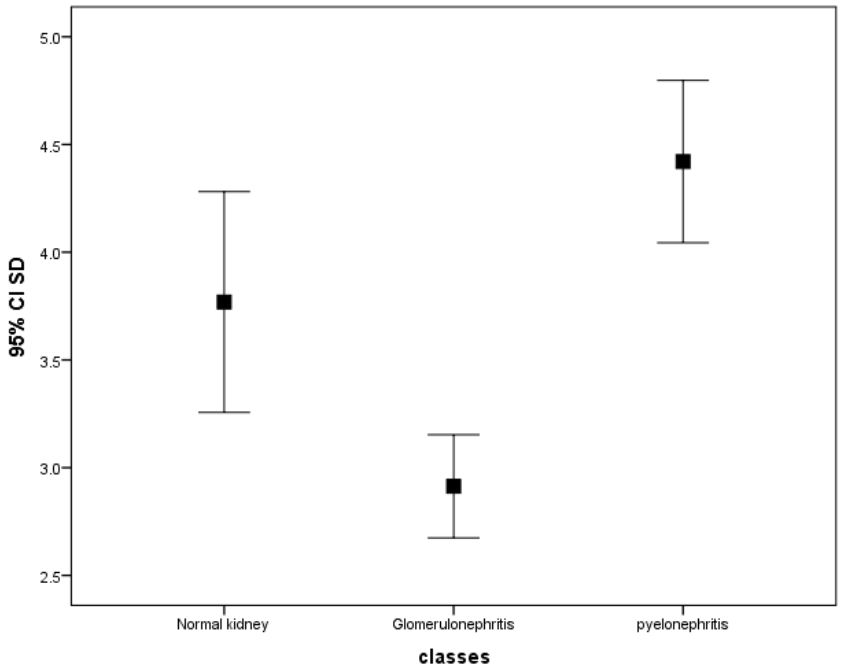
5.0
4.5
4.0
3.5
3.0
2.5
95% CI SD
Normal kidney
Glomerulonephritis
pyelonephritis
classes

(B)

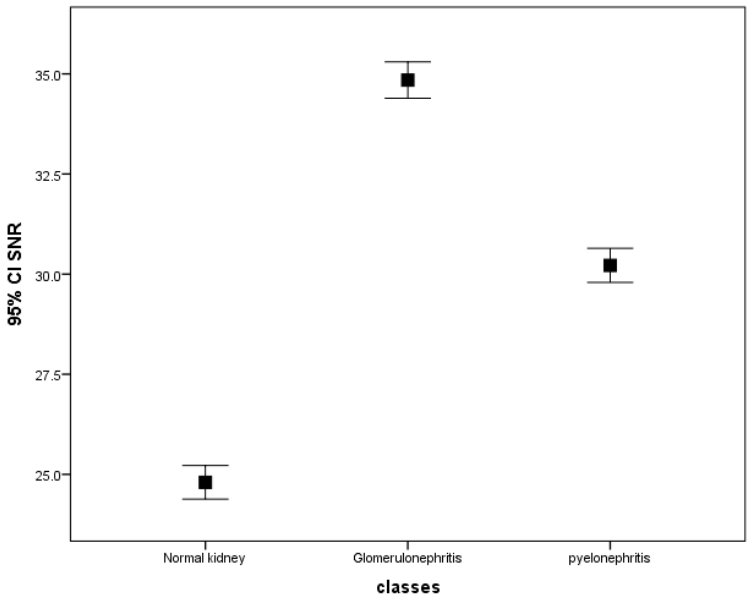

(C)

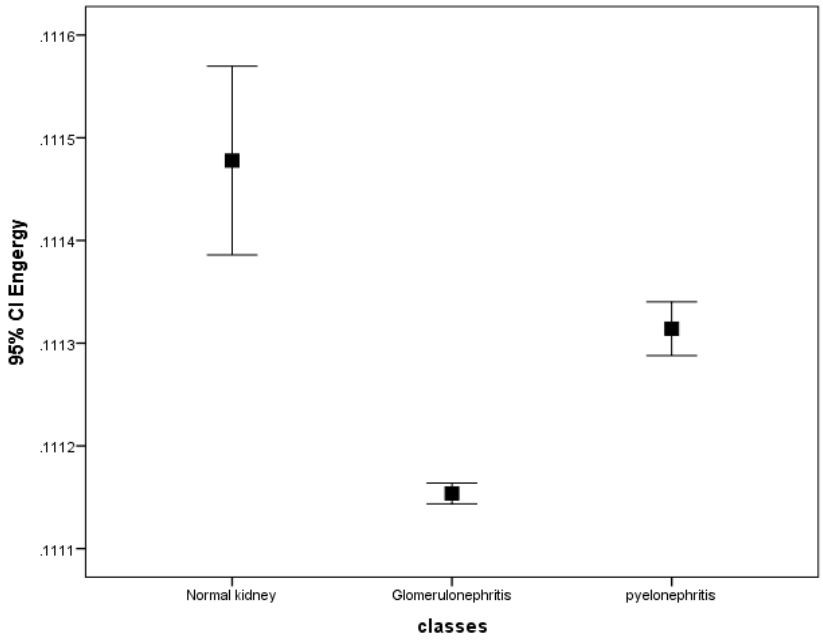

(D)

Figure 4-10 . An error bar graphs of textural features (A) mean, (B) standard deviation,(C) signal to noise ratio and (D) entropy for the different classes of the normal, glomerulonephritis and pyelonephritis pelvic calycle system of the kidneys.

Chapter Five

Discussion, conclusion and Recommendation

5-1 Discussion

A total of 234 patients were included in this study 106 were normal cases (22.6% male and 77.4% female) 128 patients had renal infections; 68 diagnosed with glomerulonephritis (38.2% males and 61.8% females) 60 with pyelonephritis (33.3% males and 66.7 females); the number of female were higher than that of male with a male to female ratio for glomerulonephritis and pyelonephritis of 1:1.6 and 1:2 respectively; which mean that females were more susceptible for renal infection than males (Figure 4-1). The patient age ranged from 11 to 80 years also indicates that infection appears in a wide spectrum of ages which might be attributed to hygiene problem. The common presenting symptoms were flank pain which appear more in patients with glomerulonephritis (Figure 4-2).

The result showed that there is a significant differences between patients with normal kidneys and those affected by glomerulonephritis and pyelonephritis in case of medical laboratory test, as well as Sonographic results at $p = 0.05$ using t-test. Sonographic appearance that showed significant differences from the normal kidney appearance includes: kidney length, corticomedullary differentiation and cortical thickness for the right and left kidney; where incase of length the infected kidney appears larger than the normal one mostly attributed to infection condition (increases of fluid content), on the other hand cortical thickness appear significantly more thinner than that of normal patient. The rest of the variable concerning the Sonographic measurement outcome showed inconclusive results they include kidney width, thickness and size for

both kidneys. Similarly laboratory investigation revealed significant differences (at p = 0.05) between patient with normal kidneys and infected one concerning RBC, WBC, Protein, and Pus cells where all these tests gives significantly higher values than those reported for patient with normal kidneys (Table4-1)

Ultrasound scanning showed that kidneys outline of 50% of pyelonephritis were hazy thick and 25% were hazy thin, where for glomerulonephritis 61.8% were smooth thin similar to normal while 20.6% showed hazy thin outline; this means pyelonephritis affected the outline of the kidneys more than glomerulonephritis because the later one affected calyces rather than medulla area (Figure 4-3).

For echotexture 58.8% of glomerulonephritis reveals hypoechogenic textures due to the presence of fluid as a result of infection, while pyelonephritis ranged from hperechogenic to hyopechogneic as well as isoechogenic depending on the stage of the disease i.e. mostly portrayed complexity in their appearance (Figure 4-4).While corticomedullary differentiation (CMD) effects appear mostly in case of pyelonephritis in which 75% of the kidneys appear with ill-defined or poor differentiation between the medulla and the cortices (Figure 4-5)

For quantitative analysis linear discriminant analysis were applied to generate regressionequation were generated(Eq. 4-1, Eq. 4-2 and Eq.4-) where the variable that correlated well with the classes (normal, glomerulonephritis and pyelonephritis) were chosen with linear discriminant analysis stepwise method; therefore it can be used to classify the patient as one of these classes according to their higher vote objectively; i.e. the equation with the highest score represent the class of interest.

In this study texture analysis were used to increase the accuracy of diagnosis using textural features extracted from medulla and pelvic calycle system for all classes. The textural feature extracted from kidney medulla showed that, the normal kidneys, and those with glomerulonephritis and pyelonephritis were classified with an accuracy of 94.9%, 97.3% and 99.5% (Table 4-3 and Figure 4-7); which means there is a heir sensitivity in classification of pyelonephritis; where it makes the medulla texture look very different than the groups, followed by glomerulonephritis which in some cases falsely classified as pyelonephritis (2.7%), with an overall classification accuracy of 98%. The most discriminant features as shown in Figure 4-8 (A, B and C) were mean, signal to noise ratio and entropy (selected by stepwise linear discriminant analysis). The textural feature mean discriminate between the normal and abnormal medulla in the kidney; where the mean signal intensity in the normal medulla were lower than that of the abnormal one; since complexity of the texture were less. Similar essence were exist in case of signal to noise ratio and entropy for the normal medulla while glomerulonephritis scored the higher textual values than pyelonephritis; which means glomerulonephritis affected textural feature of medulla more than pyelonephritis hence the textural feature of the glomerulonephritis were different than the rest of the tissues.

Also the result of classification concerning textural features extracted from the pelvic calycle system for the three groups showed overall classification accuracy of 95.7% (Figure 4-9 and table 4-4). With a higher sensitivity concerning pyelonephritis which 100% versus 99.5% for those features extracted from the medulla; this confirm that pyelonephritis texturally were very different than the other group textures. Stepwise

linear discriminant analysis selected four texture here as the most discriminant textural features. They include mean, standard deviation, signal to noise ratio and energy (Figure 4-10 A, B, C and D). Where the mean and signal to noise ratio showed an excellent separation between the three groups, while energy which represent the contrast separated glomerulonephritis from pyelonephritis well with normal pelvic calycle system showed larger variation same as the standard deviation, although the classes showed considerable separation concerning the last feature.

5-2 Conclusion

Renal infections corresponding to glomerulonephritis and pyelonephritis can be diagnosed by ultrasonography according to it is manifestations which represented by echo texture, CMD and outline of the kidney profile as well as kidney dimensions measurement like kidney length and cortical thickness, in addition to the medical laboratory test as an indicator for the presence of renal infection. The characteristics (presence of flank pain, RBC, WBC, CMD, kidney length and cortical thickness) that identify the renal infections type from the normal kidney were used in this study to identify each group objectively using linear discriminant analysis, where the classes grouped together in a class when there is a minimum between class variance while it shows maximum differences between class variance (Figure 4-6)

Normal = 81.222 - (-7.858×Flankpain) + (-0.185×RBC) + (0.001×WBC) + (15.00 ×CMD) + (12.500×Kidney length)×(17.717 × cortical thickness)

(Eq.5-1)

Glomerulonephritis = 2.308 + (-.185×Flankpain) + (.002×RBC) + (17.231× WBC) + (12.459×CMD) + (17.919× Kidney length) + (-100.147× cortical thickness)

(Eq. 5-2)

Pyelonephritis = 95.584 - (-4.745×Flankpain) + (-.065× RBC) + (.002× WBC) + (18.987×CMD) + (12.154×Kidney length) × (16.595× cortical thickness)

(Eq. 5-3)

For texture analysis Glomerulonephritis and pyelonephritis can be identified in an ultrasound image using texture analysis with an overall of accuracy of 98% using multiple linear equation developed using linear discriminant analysis from textural feature extracted from renal medulla, where the vote will be attributed to the highest score as follows:

Normal kidney = (0.099×Mean) + (221.852×SNR) + (-1.654×Entropy) - 1085.580

(Eq. 5-4)

Glomerulonephritis = (0.263×Mean) + (234.375×SNR) + (-1.712×Entropy) - 1262.280

(Eq. 5-5)

Pyelonephritis = (0.213×Mean) + (236.449×SNR) + (-1.747×Entropy) - 1252.627

(Eq. 5-6)

Similarly the same groups can be classified with an overall classification accuracy of 95.7% using texture extracted from Pelvic calycle system as follows:

Normal kidney = (1.085×Mean) + (-901.473×SD) + (271.946×SNR) + (7899815.658×Energy) - 442038.958

(Eq. 5-7)

Glomerulonephritis= (-.098×Mean) + (-904.525×SD) + (283.403×SNR) + (7907198.703×Energy) - 443071.279

(Eq. 5-8)

Pyelonephritis= (-.075×Mean) + (-901.782×SD) + (281.429×SNR) + (7895098.465×Energy) - 441673.905

(Eq. 5-9)

5-3 Recommendations

- Sinologist should look at laboratory test in case of kidney problem as well as to be aware about the flank pain to pay attention to the characteristics of glomerulonephritis and pyelonephritis from normal

- Sinologist should report the condition of cortical thickness, kidney length, CMD and kidney outline as routine in renal scan.

- Linear discriminant analysis equation concerning laboratory test and ultrasonography characteristics of the kidney should be incorporated in quantitative scoring.

- Texture analysis can be integrated in ultrasonography as Computer Aided Diagnosis method to reduce the operator dependent concept in ultrasound field and hence reduce variability of judgment.

- Further study can be done incorporated blood flow indices (Doppler)

References

Abdoelrahman H A. B., Adil A. Mansour, M. E. M. Gar-elnabi,Elsir Ali Saeed, Ultrasonographic Renal Length and Parenchymal Thickness in Normal Sudanese Population, International Journal of Science and Research (IJSR) ISSN

Al-KhaderAA,Tamim H, SulaimanMH,JondebyMS,TaherS,Hejaili FF, et al.what is the most appropriate formula to use in estimating glomerular filtration rate in adult Arabs without kidney disease? Ren Fail 2008;30:205-8.

B. Chevaillier, B. Ponvianne, J. L. Collette, D. Mandry, M. Claudon, & O. Pietquin, (2008).Functional semi-automated segmentation of renal DCE-MRI sequences. In Proceedings of the IEEE International Conference on Acoustics, Speech and Signal Processing (ICASSP) (pp. 525-528).

B. van Ginneken, S. Katsuragawa, and B. terHarrRomeny, "Automatic detection of abnormalities in chest radiographs using local texture analysis", IEEE Trans Med Imag., Vol.21(2), 2002, pp.139-149.

Brandt TD,NeimanHL,DragowskiMJ,Bulawa W ,ClaykampGUltrasound assessment of normal renal dimensions Journal Ultrasound Med.1982 Mar,L(2):49-52.

Brown, P. (2003) Ultrasound in Diffuse Renal Disease. British Medical Ultrasound Society Bulletin, 11, 30-35.http://ult.sagepub.com/content/11/4/30.full.pdf

C.A.Binkert,U.Hoffman,D.A.Leung,H.G.Matter.M.Schmidt,J.F.Debatin

A.Characterization of renal artery stenoses based on magnetic resonance renal flow and volume measurements. Kidney Int56:1846-1854,1999.

Carol et aL; Diagnostic ultrasound imaging .sonographic technique 2011,4th edi,9-321.

C.U .McRae, F.T. Shannon, Utley WLF.Effect on renal growth of re implantation of refluxing ureter.Lancet 1974; 1:1310-1312.

Cockcroft DW, Gault MH. Prediction of creatinine clearance from serumcreatinine. Nephron 1976;16:31-41.

Dean D. Buirwin Institute of Diagnostic Medical Ultrasound. Obstetrical ultrasound 2002,(1-3)197-214.

D.Miletic ,Z.Fuckar, A.Sustic,V.Mozetic,D.Stimac, G.Zauhar: Sonographic measurement of absolute and relative renal length in adults. JClinUltrasound26 : 185-189,1998.

D.-Y. Kim and J.-W. Park, "Computer-aided detection of kidney tumor on abdominal computed tomography scans", ActaRadiol. Vol.45, 2004, pp.791-795.

Emamian SA, Nielsen MB,Pedersen JF.:Intaobserver and Interobserver variations in sonographic measurements of kidney size in adult volunteers. ActaRadiol 36:399-401,1995.

Fontanilla T, Minaya J, Cortés C, Hernando CG, Arangüena RP, Arriaga J, Carmona MS, Alcolado A. Abdom Imaging. 2012 Aug;37(4):639-46. doi: 10.1007/s00261-011-9781-2.PMID: 21792579

G ItalNefrol. Ultrasound assessment in renal infections, 2012 Nov-Dec;29Suppl 57:S47-57.

G.N. Lee, X. Zhang, and M. Kanematsu et al.,"Classification of cirrhotic liver on MR images using texture analysis", Int'l J. CARS, Vol.1, Supp. 1, 2006, pp.379-381.

Gehan EA, George SL: Estimation of human body surface area from height and weight. Cancer Chemother Rep 54: 225–235, 1970.

Glodny B, Unterholzner V, Taferner B, (2009. "Normal kidney size and its influencing factors - a 64-slice MDCT study of 1.040 asymptomatic patients". BMC Urology 9: 19. doi:10.11861471-2490-9-19. PMC 2813848.

Goldenberg RL, Cutter GR,HufferHJ,NelsonKG,Hauth JC. Intrauterine growth retardation :Standard for Diagnosis.AMJ obstetric Gynecol 1989;161;271-277.

HAROLD, E. 2006. Clinical Anatomy :Applied anatomy for students and junior doctors, Oxford, Blackwell Publishing Ltd.

Hendee,WR.Medical imaging physics 4th Ed. New York (NY): Willey less; 2002.P.10.

H. K. Koh, S. W. Shen, B. Shuter, & A. A. Kassim, (2006).Segmentation of Kidney Cortex in MRI Studies using a constrained Morphological 3D H-maxima Transform. In Proceedings of the 9th International Conference on Control, Automation, Robotics and Vision, (ICARCV), (pp. 1-5).

H. Yoshida, D. Casalino, and B. Keserci et al., "Wavelet packet based texture analysis for differentiation between benign and malignant liver tumors in ultrasound images", Phys. Med. Biol. Vol. 48, 2003, pp.3735-3753.

Ho SikShin,Byung Ha Chung,SangEun Lee, Woo Jin Kim,Hong Il Ha, and Chul Woo Yang, Measurement of kidney volume with MDCT in young Korean.

H-P. Chan, B. Sahiner, and N. Petricket. al. "Computerized classification of malignant and benign microcalcifications on

mammograms: texture analysis using an artifical neural network", Phys. Med. Biol., Vol. 42, 1997, pp.549-567.

Jan A. Bates; MPH;L DMU ;DCR;abdominal Ultrasound. 2nd Edition 2004; P .1.

J. Xie, Y. Jiang, & H. Tsui (2005). Segmentation of kidney from ultrasound images based on texture and shape priors.IEEE Trans. on Medical Imaging, (Vol. 24).

J.Bakker, M.Olree, R .Kaatee, E.E. de Lange, K.G Moons, J.J. Beutler, F.J.Beek: Renal volume measurements: Accuracy and repeatability of US compared with that of MR imaging. Radiology211 :623-628,1999.

J.R. Wilkie, M.L. Giger, and M.R. Chinander,"Comparison of radiographic texture analysis from computed radiography and bone densitometry systems", Med. Phys. Vol.31, 2004, pp.882-891.

Joel Neugarten ,BertamKasiske, Sharon R, Silbiger , Jens R.Nyengaard Effects of sex on Renal Structure,Nephron 2002;90:139-144.

KEMP., W., BURNS., D. & BROWN., T. 2008. Pathology: The Big Picture, McGraw-Hill Companies.

Kfar Saba. Isr Med Assoc J. 2007 Oct;9(10):729-31 Rathaus V(1), Werner Medical Imaging, Acute focal nephritis

K.KirkShung. Medical imaging physics 4th Ed. Raton London NEW YORK (NY): CRC press; 2002.P. 308-310.

L. Lan, M.L. Giger, and J. R. Wilkie et al., "Automated selection of region of interest for radiographic texture analysis", Proc SPIE Medical Imaging, Vol. 6514, 2007, pp.651436

Kiw-Yong Kang, Young JoonLee,SoonChul Woo Yong-SooKim,In Sung Moon,Yong Bok Koh,ByungKee Bang and Bum Soon Choi A comparative study of methods of estimating kidney length in kidney

transplantation donors.OxfordJournals,Medicine,,NephrologyDialsis Transplantation, Volume22, Issue 8,Pp.2322-2327.

M. Marcuzzo, P. R. Masiero, & J. Scharcanski, (2007). Quantitative Parameters for the Assessment of Renal Scintigraphic Images, Engineering in Medicine and Biology Society, 2007.

MCMINN, R. M. H. 2009. Last's Anatomy Regional and Applied, Edinburgh, Churchill Livingstone.

M. Zhang, M.L. Giger, and K. Doi, "Mammographic texture analysis for the detection of spiculated lesions", In: 3rd Int'l Workshop on Digital Mammography (eds. K. Doi, M. L. Giger, R. M. Nishikawa, R. A. Schmidt), Elsevier Science, Amsterdam, pp. 347-350, 1996.

M.Absy, C .Metreweli, C. Matthews, A. Al Khader.Changes in transplanted kidney volume measured by ultrasound.Br J Radiol 1987; 60:525-529.

M.R. Chinander, M.L. Giger, and R.D. Shah et al., "Investigation of using bone texture analysis on bone densitometry images", Proc SPIE, Vol. 4684, 2002, pp.860-863, 2002.

Mahajan S, MukhiyaGK,Singh R , TiwariSC,KalraV,Bhowmik DM, et al. Assessing glomerular filtration rate in healthy Indian adults : A comparision of various prediction equatuions. J Nephrol2005 ; 18:257-61.

N.R. Mudigonda, R.M. Rangayyan and J.E.L. Desautels,"Gradient and texture analysis for the classification of mammographic masses", IEEE Trans. Med. Imag., Vol.19(10), 2000, pp.1032-1043.

P.Allan :The normal kidney. In :Clinical Ultrasound : A Comprehensive Text, 2nd Ed., edited by Meire H , Cosgrove D,DewburyK,Farrant P ,NewYork, Churchill Livingstone,2001,pp513-528.

R. Gupta and P.E. Undrill, "The use of texture analysis to delineate suspicious masses in mammography", Phys. Med.

Biol. Vol.40, 1995, pp.835-855

Robert Barkow, MD ., Mark H, Beers M,D .MARK MANUAL of medical information 2009.

R. M Haralick,. 1979. Statistical and structural approaches to texture. Proceedings on the IEEE (67) 5: 786-803.

R. M Haralick., K. Shanmugam& I. Dinstein. 1973. Textural feature for image classification. IEEE Trans. Man, Cybern, 6:610-621.

R.H. Dean, R.W .Kieffer, B.M. Smith, et al. Reno vascular hypertension, anatomic and renal function changes during drug therapy. Arch Surg 1981; 116:1408-1415.

R.H.Breau, E.Clark ,B.Bruner,P,Cervini,T.Atwell,G.Knoll,B.C.Leibovich Simple method to staminate renal volume from CT .Can UrolAssoc J,2013 May-jun;7(5-6) :189-92.doi:10.5489/cuaj.1338.

R.J. Bartrum, E.H .Smith, C.J. D'Orsi, J .Dantono. The ultrasonic determination of renal transplant volume . JCU 1974; 2:281-285.

S .Troell, U. Berg, B. Johonsson, I .Wikstad.Ultrasonographic renal parenchymal volume related to kidney function and renal parenchmal area in chlden with recurrent urinary tract infections and asymptomatic bacteriuria. ActaRadiol 1984:25:411-416.

S. Poonguzhali, and G. Ravindran (2008), Automatic Classification of Focal Lesions in Ultrasound Liver Images Using Combined Texture Features. Information Technology Journal**.**

S. Sahiner, H.-P. Chan, and N. Petrick et al.,"Computerized characterization of masses on mammograms: the rubber band straightening transform and texture analysis", Med. Phy. Vol.25(4), 1998, pp.516-526.

S.A Emamian, M.B Nielsen, J.F Pedersen, L. Yite:Kidney dimensions at sonography:Correlation with age, sex, and habitus in 665 adult volunteers. AJR Am J Roentgenol1601 :83-86,1993.

Samuel Johnson , Rahul Rishi,Andreea And one, WassimKhawandi , Gafar Al-Said,NanaGletsu-Miller, Edward Li n ,Deborah A.Baumgarten , and W, Charles O'Neil Determination and Functional Significance of Renal parenchymal Volume in AdultsCin J Am Soc Nephrol.2011 January;6(1):70-76.

Sargent MA ,LongG,KarmaliM,Cheng SM:.Interobserver variation in the sonographic estimation of renal volume in children. PeditrRadiol 27:663-666, 1997.

Snell , Clinical Anatomy By System ,Lippincott Williams &Wilkins 2007.

SNELL, R. S. 2005. Clinical Anatomy for Medical Students, Philadelphia, Lippincott Williams and Wilkins.

T.B. Jones, L.R. Riddick, M.D. Harpen, R.L .Dubuisson, D. Samuel. Ultrasonographic determination of renal mass and renal volume .J Ultrasound Med 1983;2:151-4.

T.D Brandt, H.L.Neiman, M.J.Dragowski, W.Bulawa,G.Claycamp : Ultrasound assessment of normal renal dimensions.J Ultrasound Medl :49-52,1982.

Tempkin, B. B. 1999. Ultrasound scanning : principles and protocols, Philadelphia, W.B. Saunders Co.

Tortora, G. J. &B. Principles of ANATOMY & PHYSIOLOGY, USA, Biological Science Textbooks.2012

V.thakur. T.Walkins,K.McCarthy, T.Beidl,N.Underwood,K.Barnes,E.M. Cook: Is kidney length a good predictor of kidney volume ?Am J Med Sci313 :85-89,1997.

Watson PE, Watson ID, Batt RD: Total body volumes for adult males and females estimated from simple anthropometric measurements. Am J ClinNutr 33: 27–39, 1980.

Wan MahaniHafizah, EkoSupriyanto, JasmyYunus, Feature Extraction of Kidney Ultrasound Images based on Intensity Histogram and, 978-0-7695-4730-5/12 $26.00 © 2012 IEEE DOI 10.1109/AMS.2012.47

Werner S Harmse Normal variance in Renal size in relation to body habits,South African Journal of Radiology,Vol 15,Noa(2011).

Widjaja E, OxtobyJW,Hale TL, Jones PW, Harden PN, McCall IW. Ultrasound measured renal length versus low dose CT volume in predicting single kidney glomerular filtration rate .Br J Radiol 2004;77:759-64.

William V. Raszka, Jr, MD,* Omar Khan, Sonographic assessment of pyelonephritis MD October 2005

X. Chen, K. Doi, and S. Katsuragawa et al., "Automated selection of regions of interest for quantitative analysis of lung textures in digital chest radiographs", Med. Phys., Vol.20, 1993, pp.975-982.

Appendix (A) Ultrasound images

image. (A-1) : coronal view of right kidney in a 14-year old male patient with normal
findings

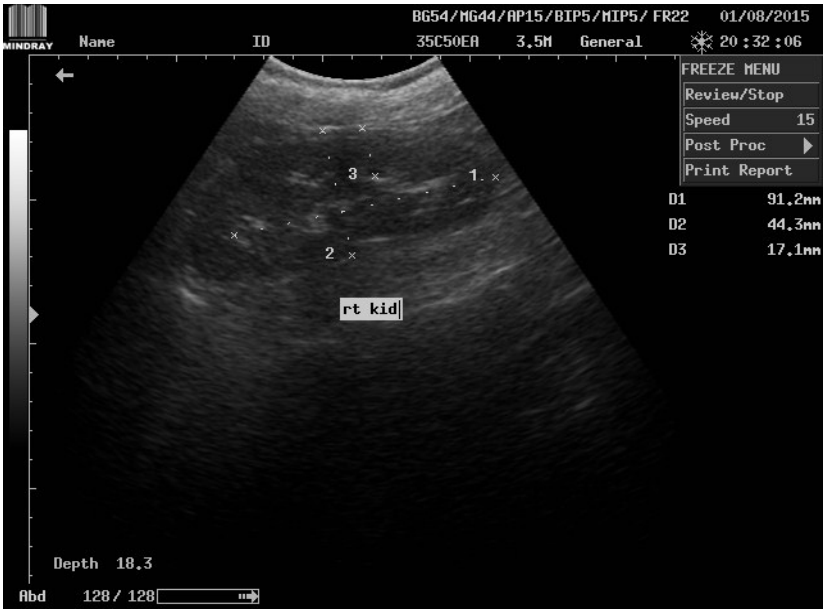

image. (A-2) : coronal view of right kidney in a 53 -year old female patient with normal finding

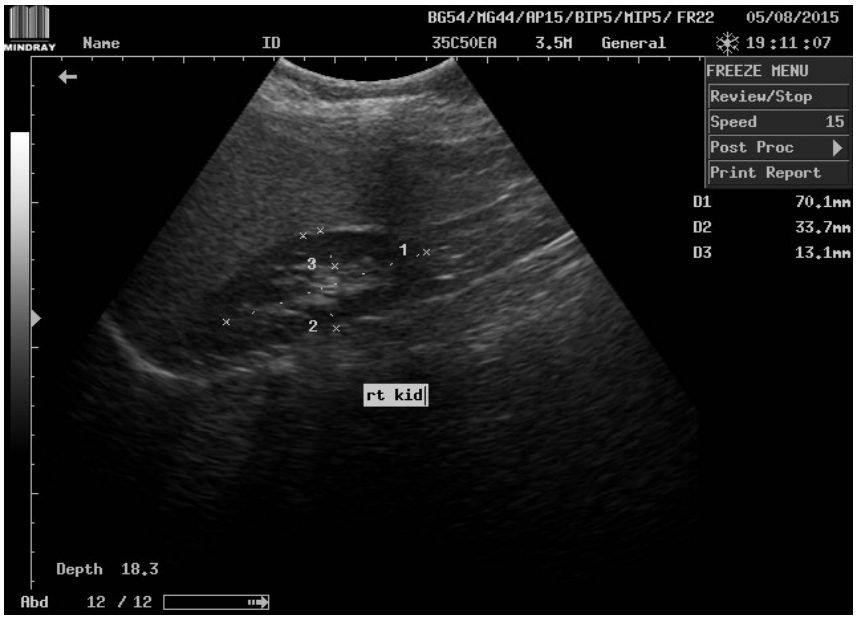

image. (A-3) : coronal view of right kidney in a 17-year old female patient with normal findings

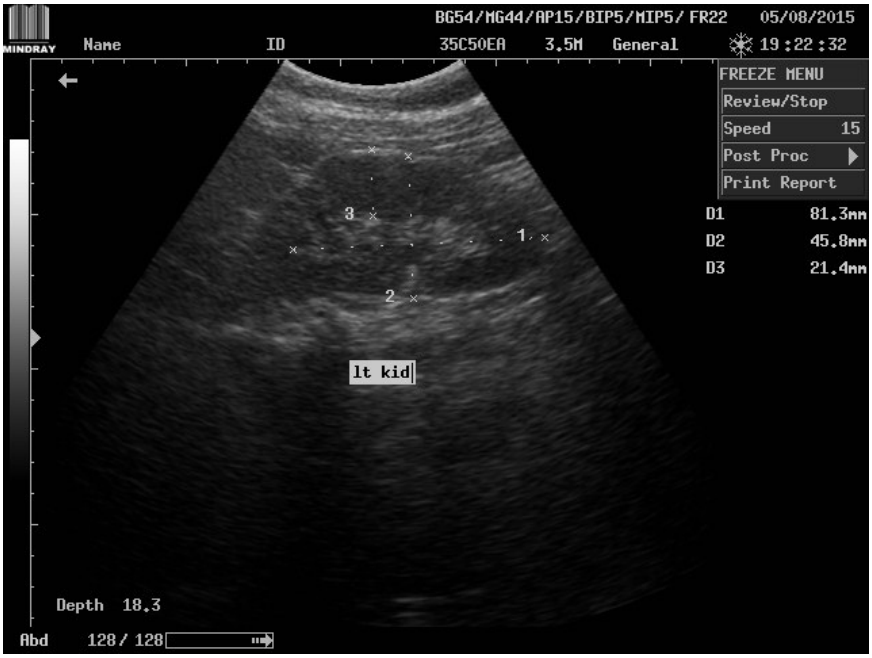

image. (A-4): coronal view of left kidney in a 47-year old female patient with normal

Findings

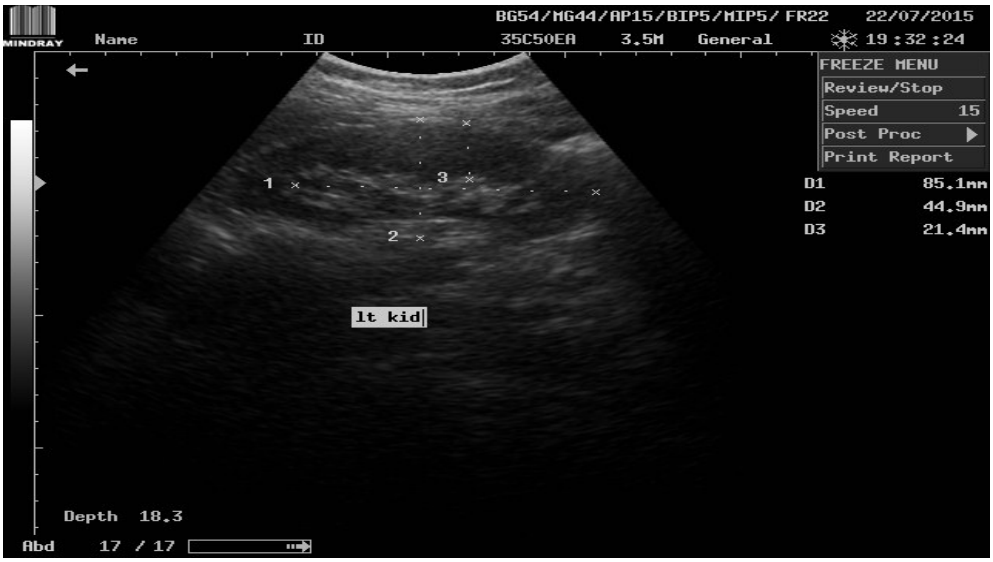

image. (A-5): coronal view of left kidney in a 44-year old female patient with normal

Findings

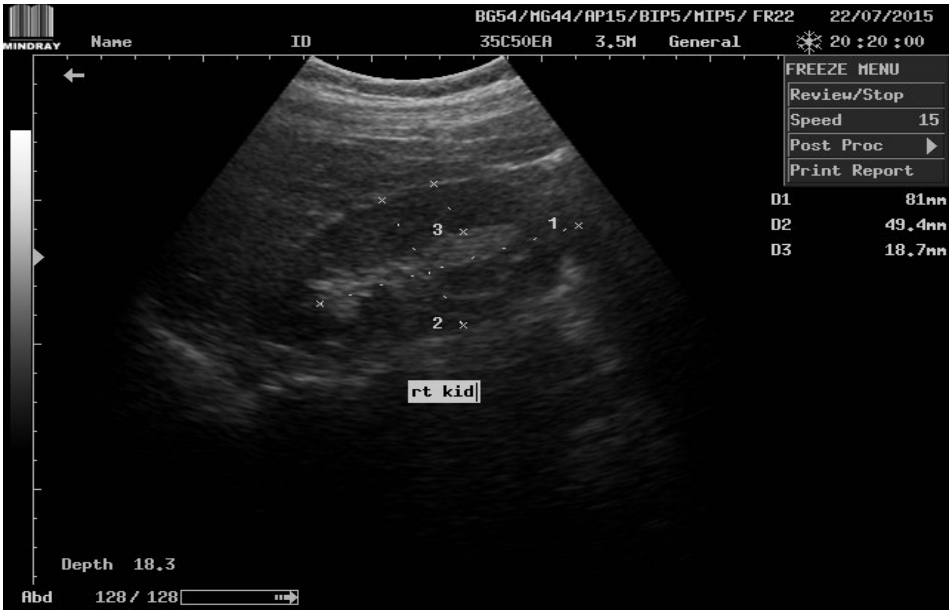

image. (A-6): coronal view of right kidney in a 48-year old male patient with normal

Findings

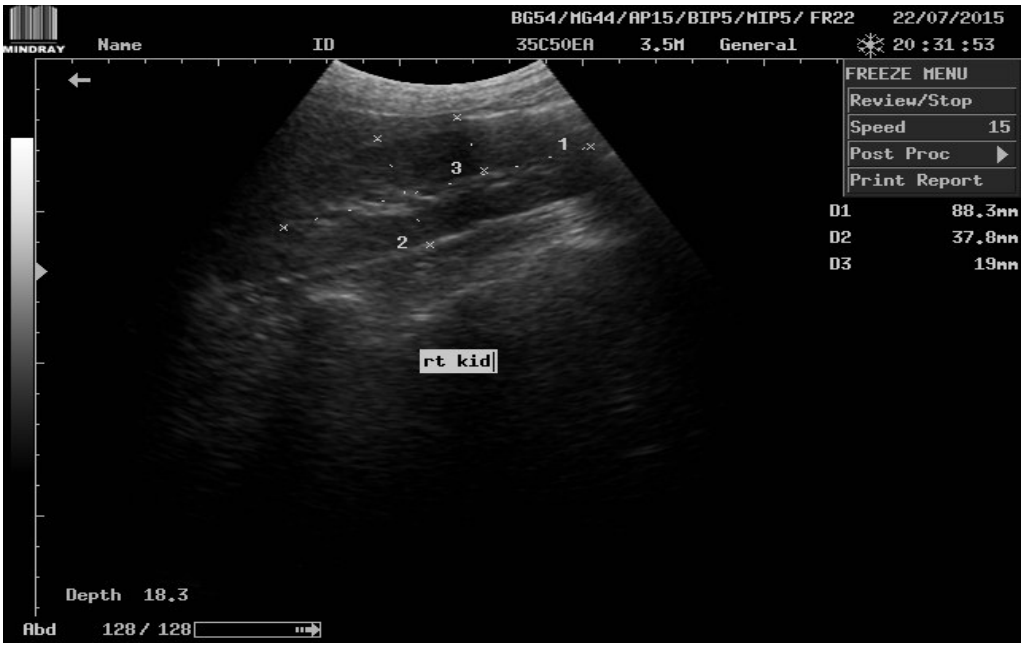

image. (A-7): coronal view of right kidney in a 35-year old male patient with normal

Findings

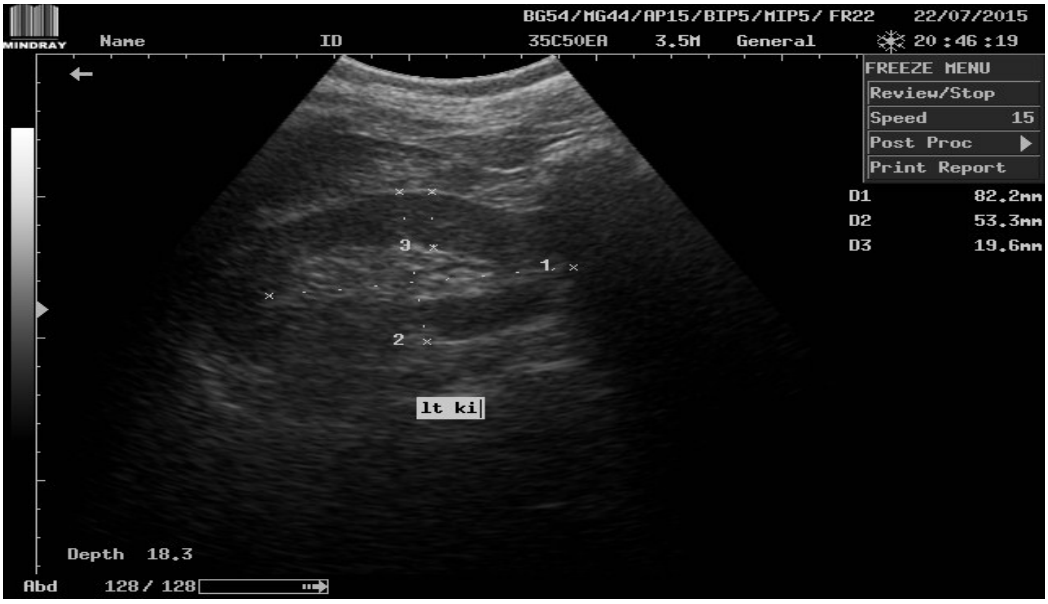

image. (A-8): coronal view of left kidney in a 54-year old male patient with normal

Findings

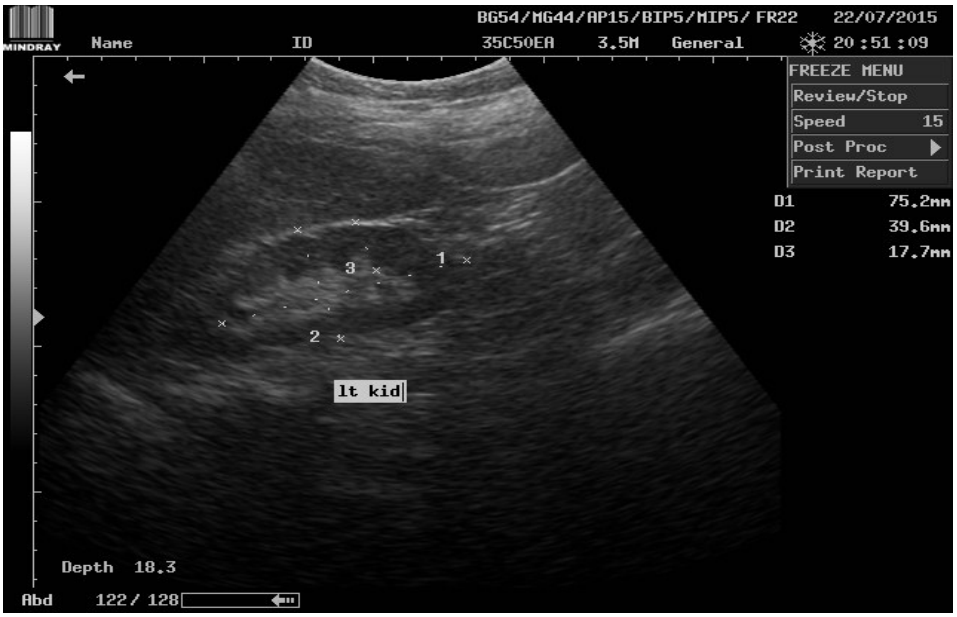

image. (A-9): coronal view of left kidney in a 57-year old female patient with normal

Findings

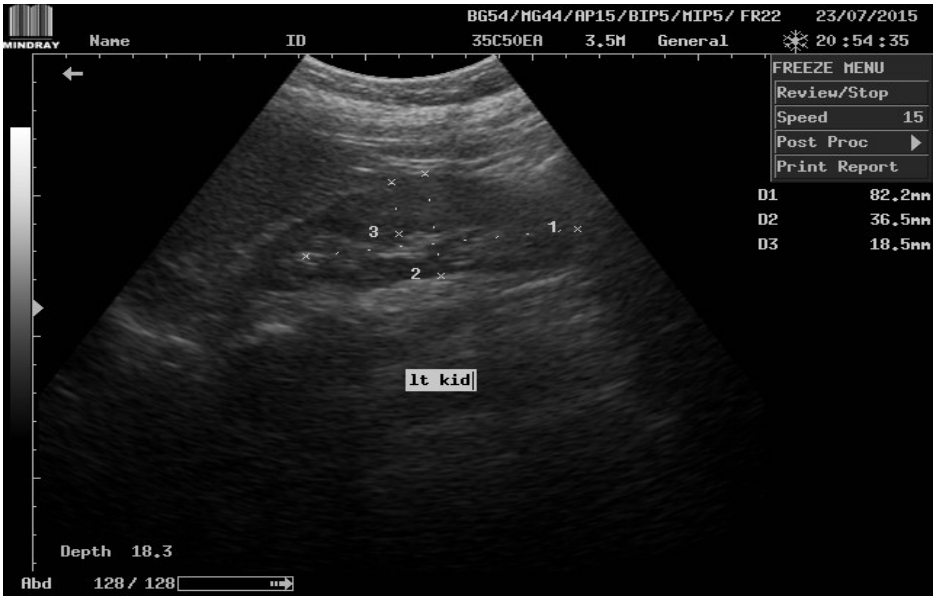

image. (A-10): coronal view of left kidney in a 37-year old female patient with normal

Findings

image. (A-11): coronal view of right kidney in a 49-year old male patient with normal

Findings

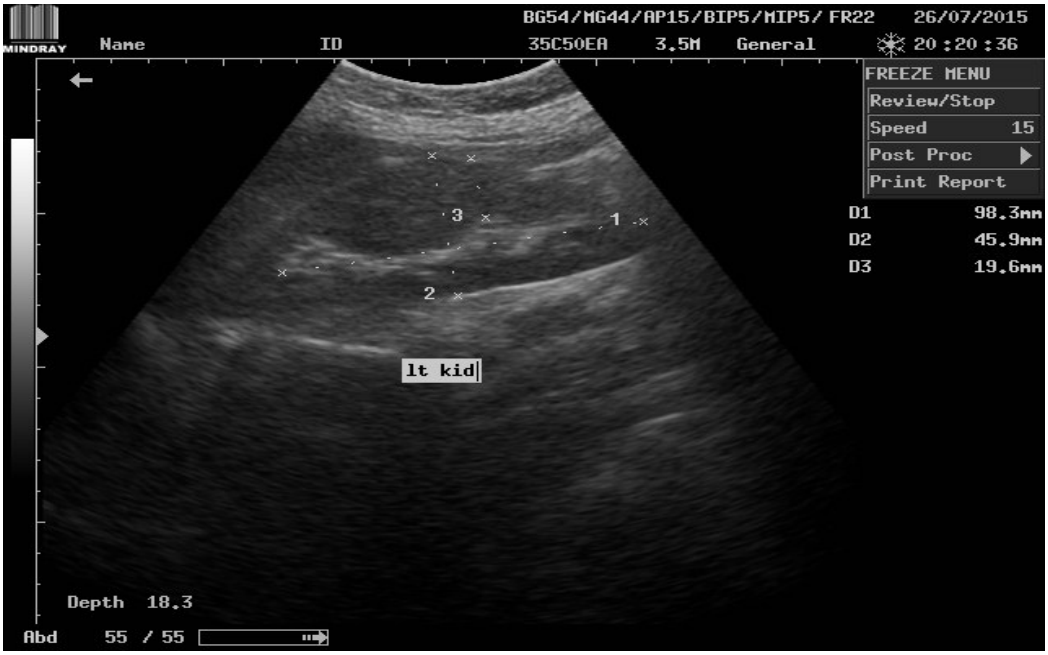

image. (A-12): coronal view of left kidney in a 17-year old female patient with normal

Findings

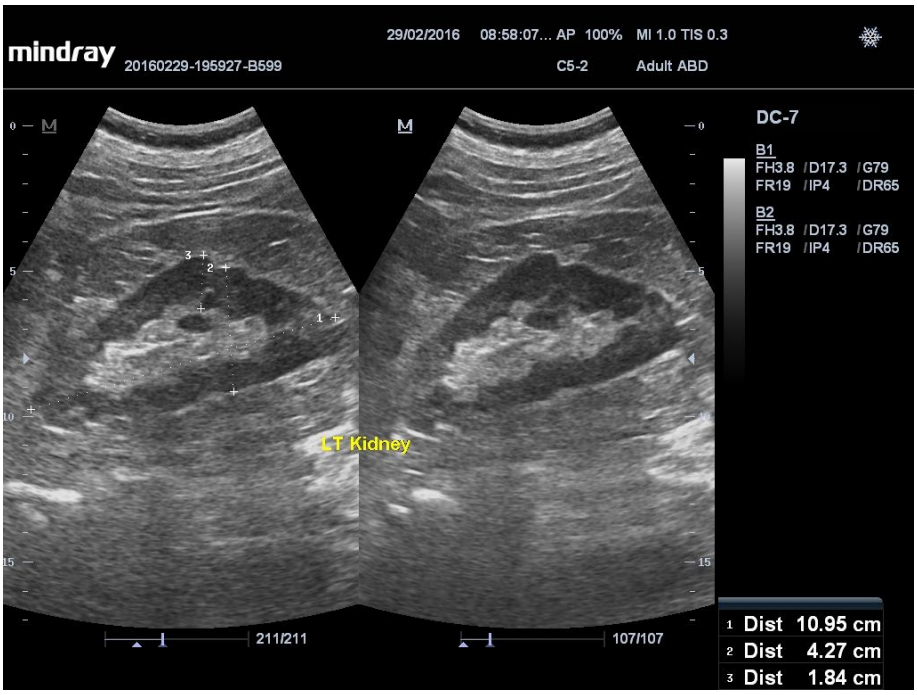

image. (A-13): coronal view of left kidney in a 25-year old female patient with glomerulonephritis

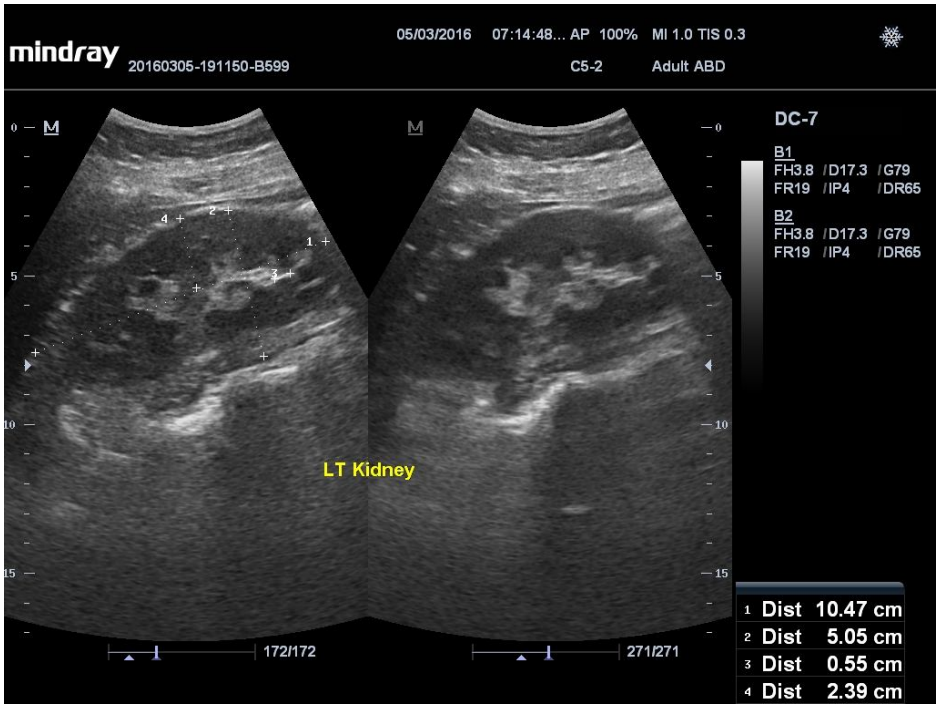

image. (A-14): coronal view of left kidney in a 20-year old female patient with glomerulonephritis

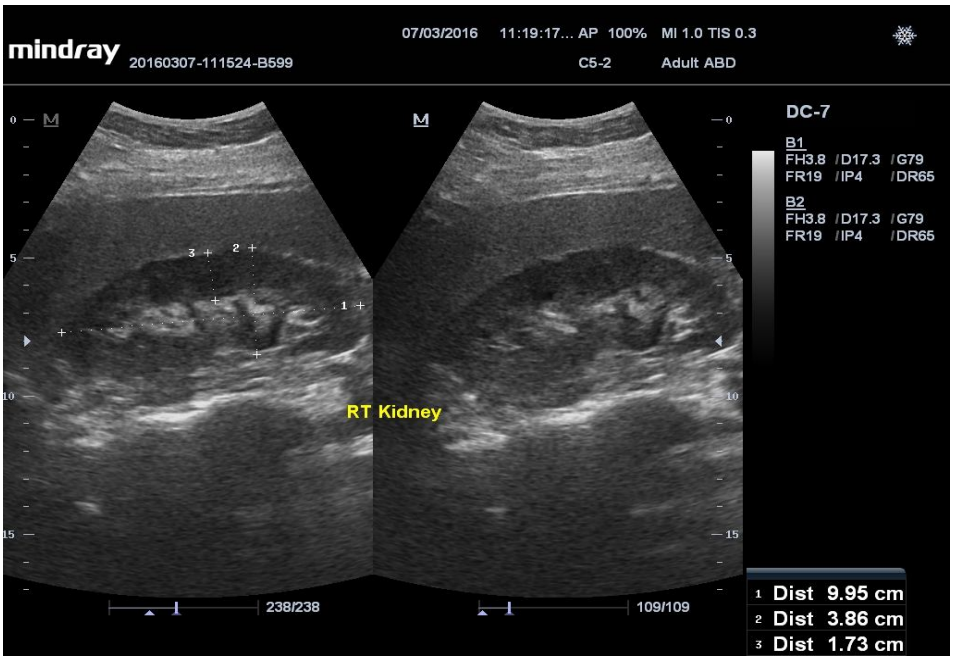

image. (A-15): coronal view of right kidney in a 22-year old male patient with glomerulonephritis

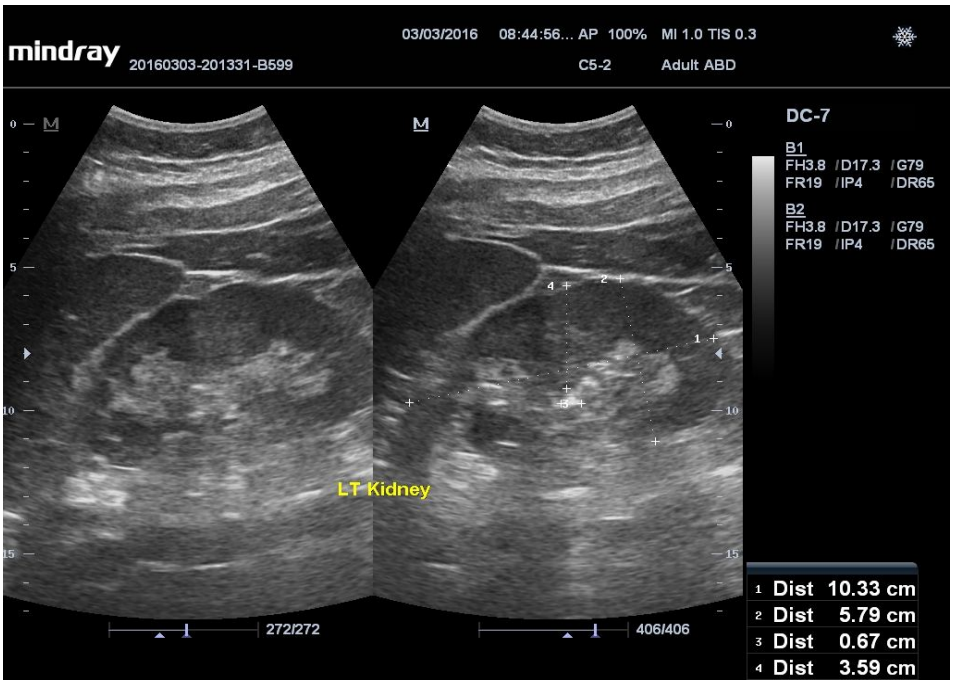

image. (A-16): coronal view of left kidney in a 29-year old female patient with glomerulonephritis

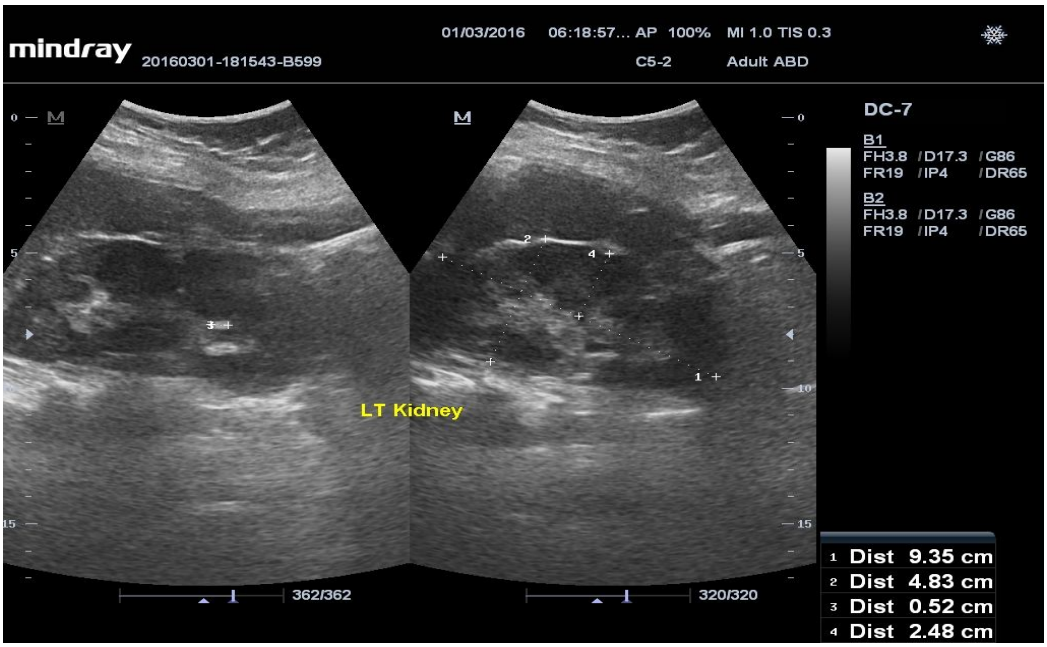

image. (A-17): coronal view of left kidney in a 28-year old male patient with glomerulonephritis

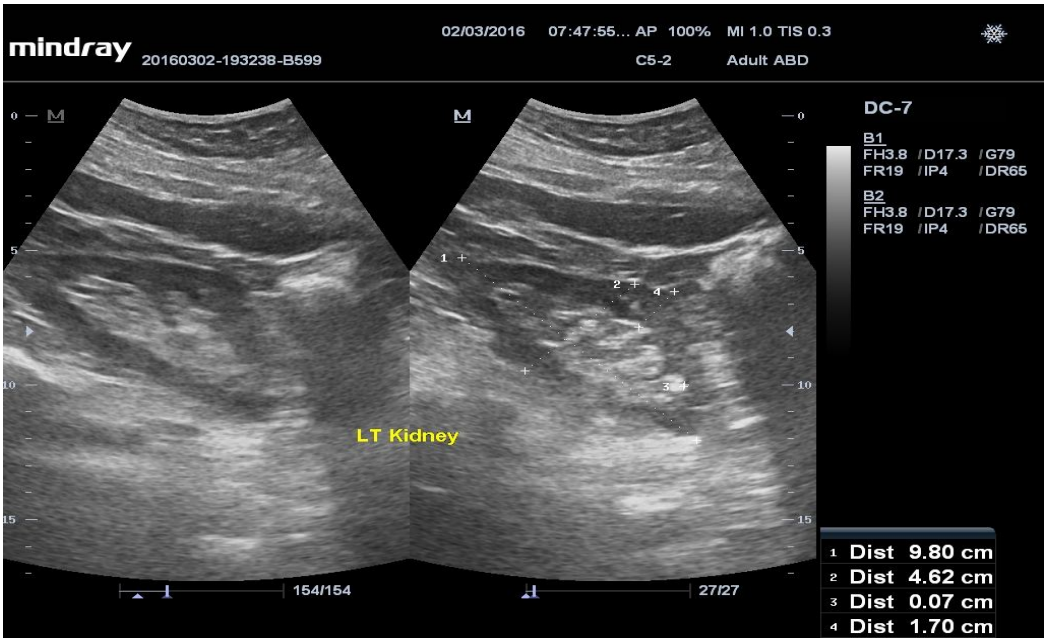

image. (A-18): coronal view of left kidney in a 19-year old male patient with glomerulonephritis

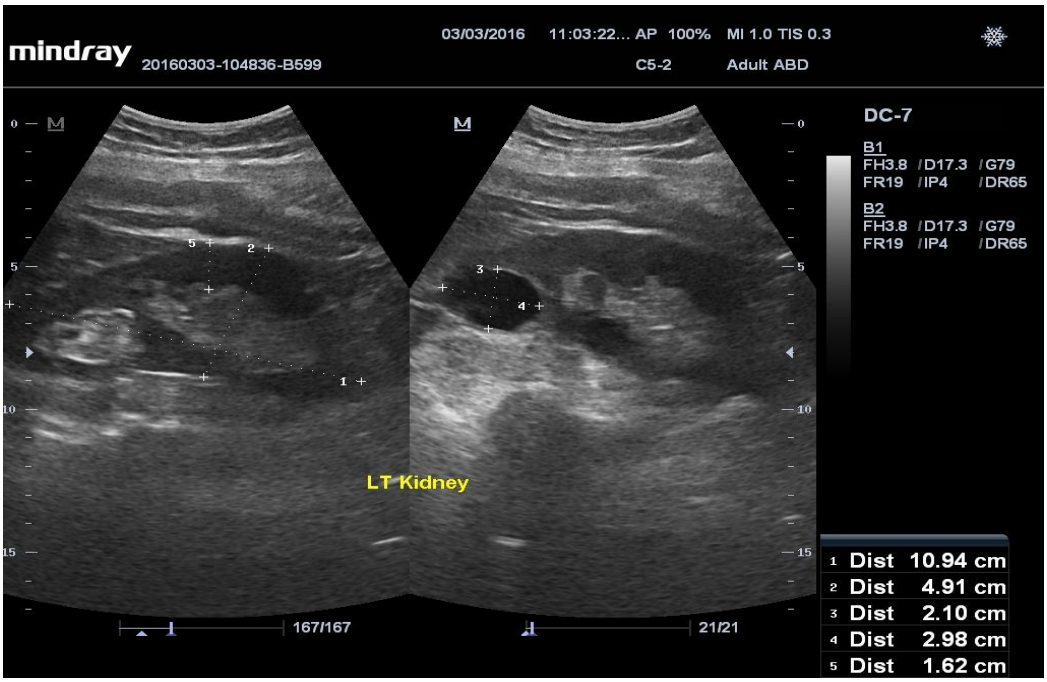

image. (A-19): coronal view of left kidney in a 61-year old female patient with glomerulonephritis

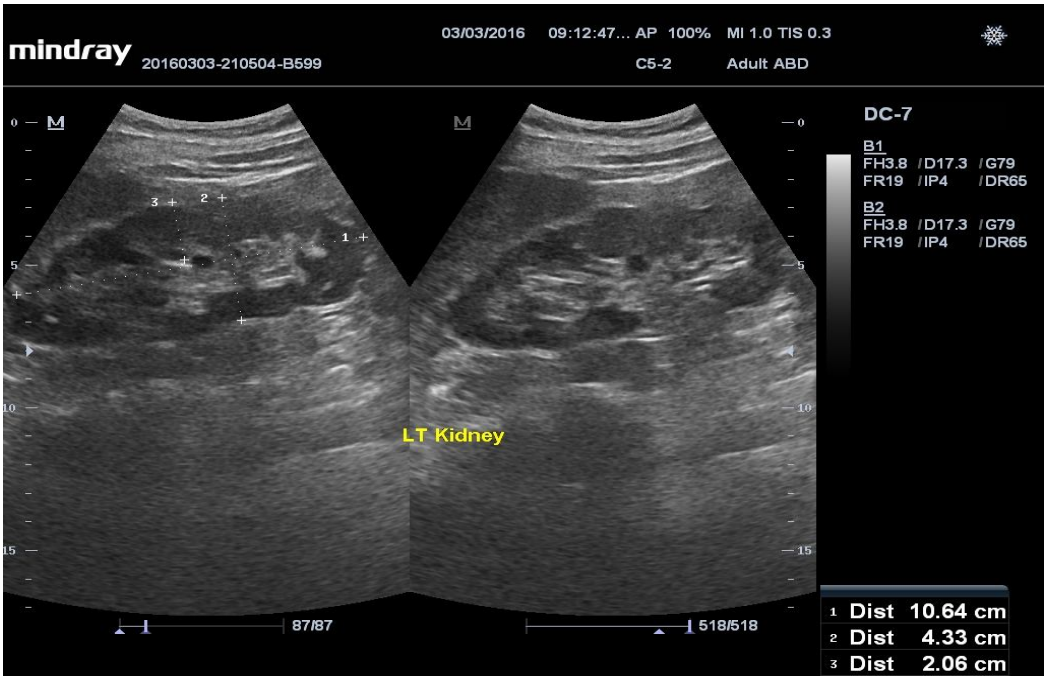

image. (A-20): coronal view of left kidney in a 22-year old female patient with glomerulonephritis

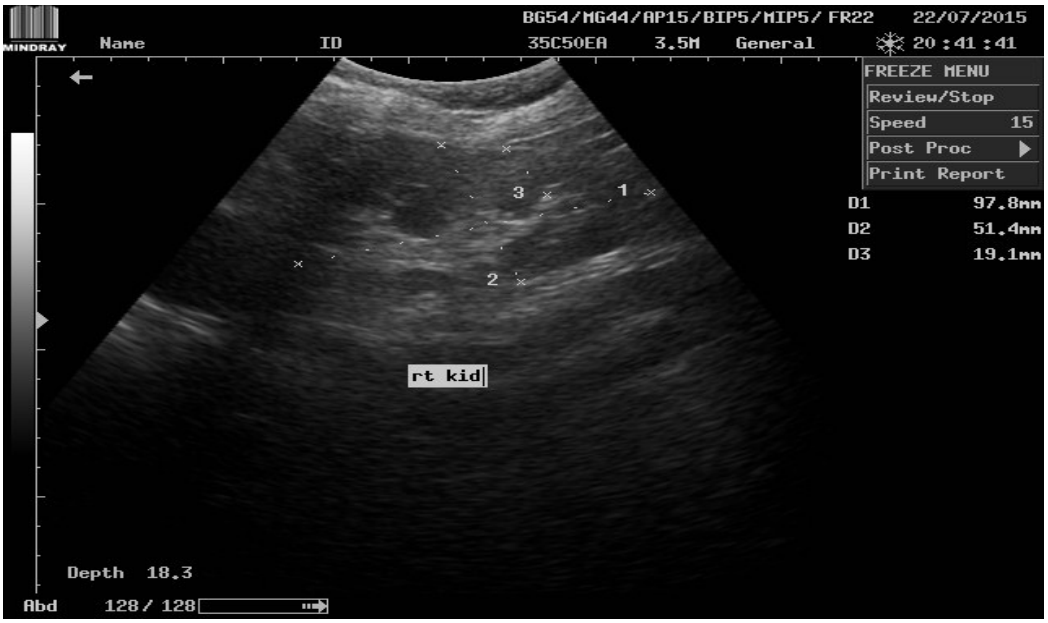

image. (A-21): coronal view of right kidney in a 50-year old female patient with glomerulonephritis

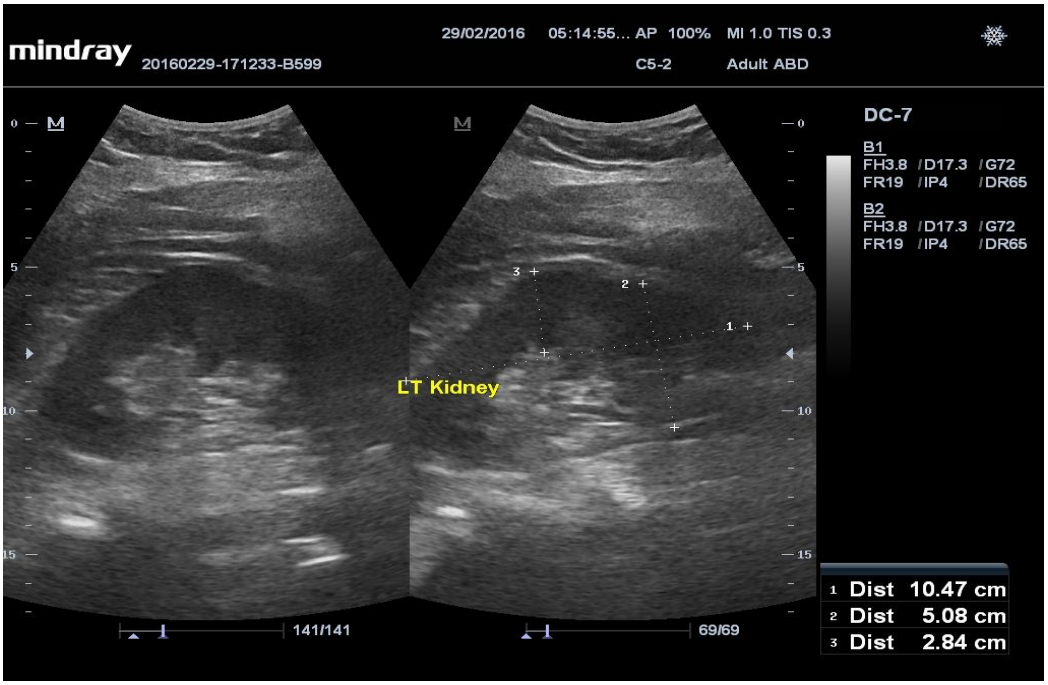

image. (A-22): coronal view of left kidney in a 18-year old female patient with glomerulonephritis

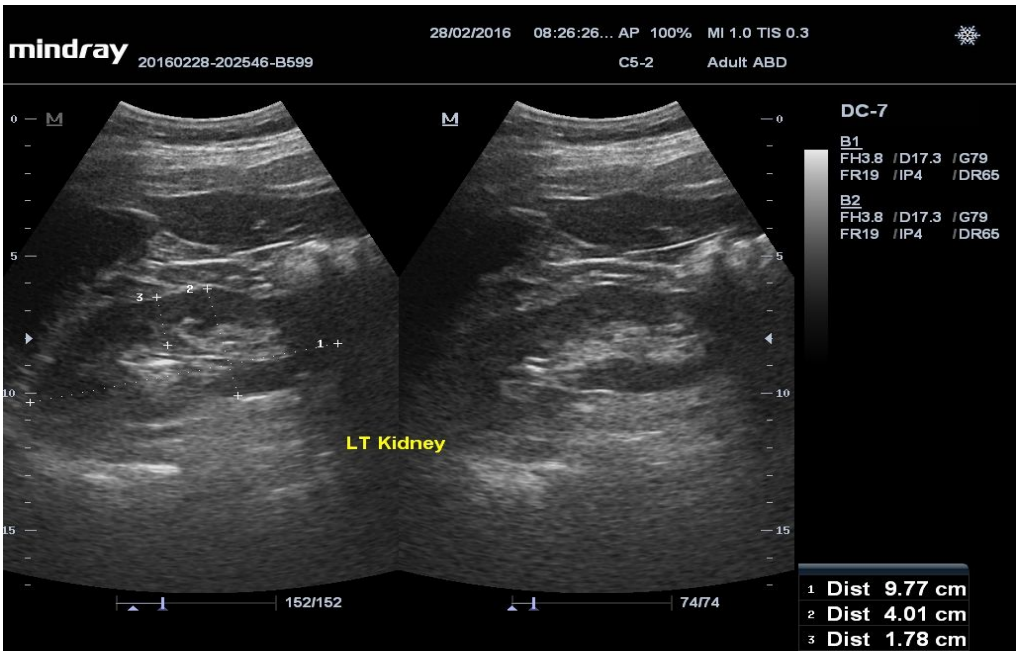

image. (A-23): coronal view of left kidney in a 42-year old female patient with glomerulonephritis

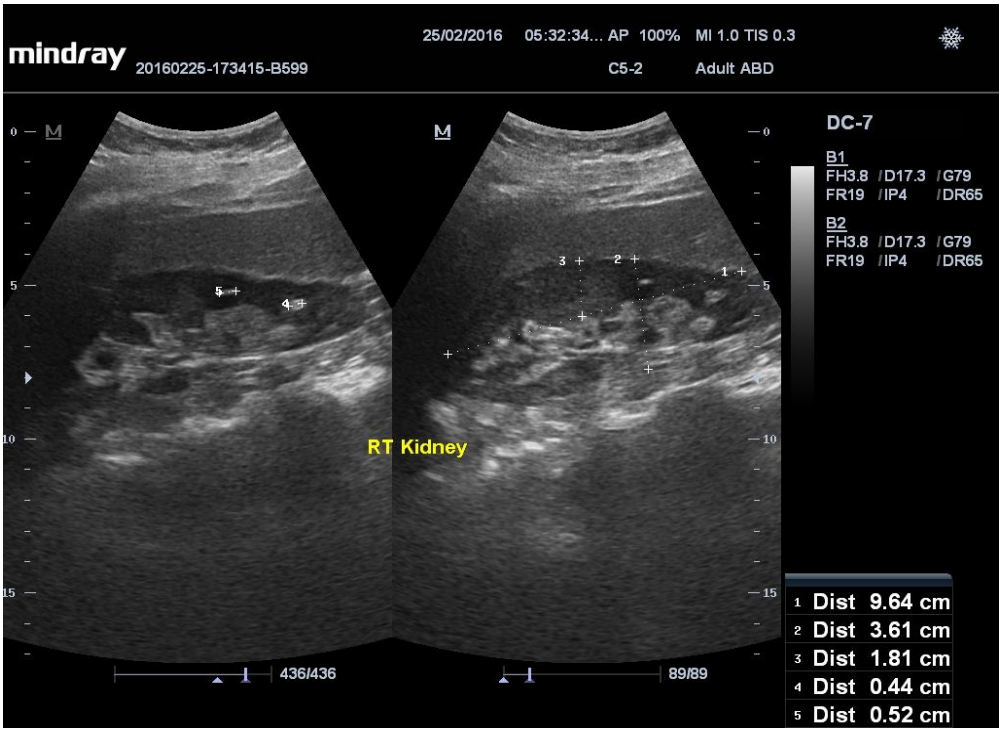

image. (A-24): coronal view of right kidney in a 28-year old female patient with glomerulonephritis

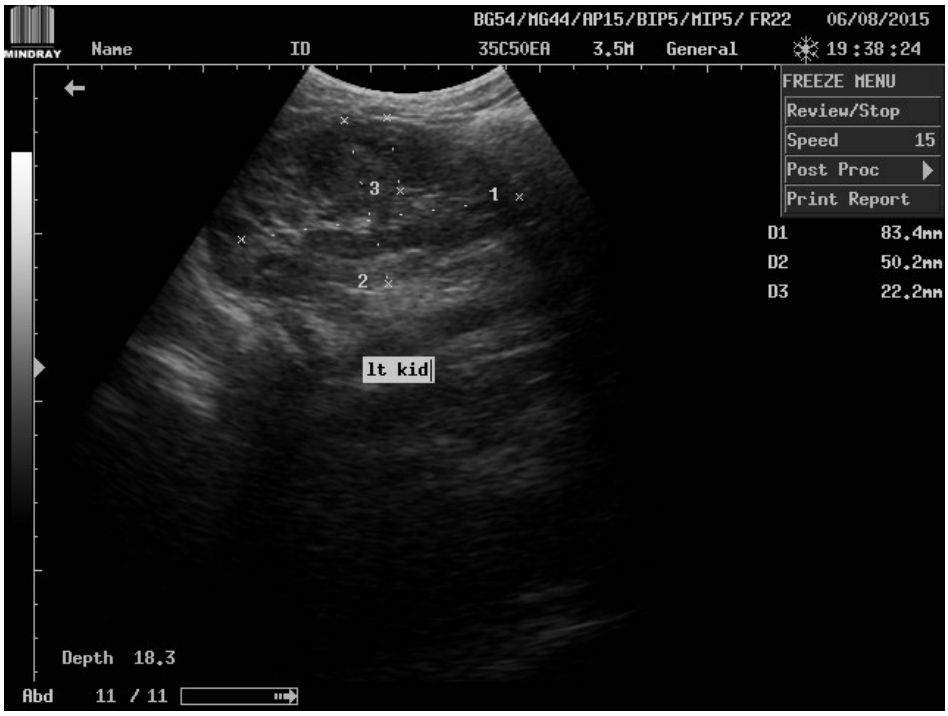

image. (A-25): coronal view of left kidney in a 43-year old male patient with pyelonephritis

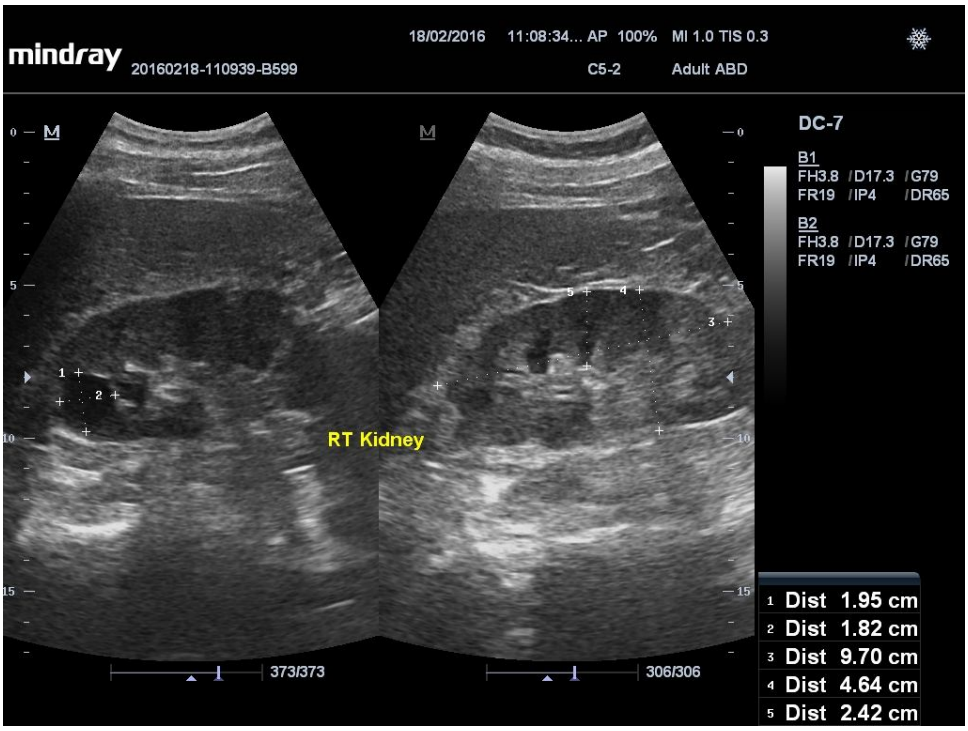

image. (A-26): coronal view of right kidney in a 57-year old female patient with pyelonephritis

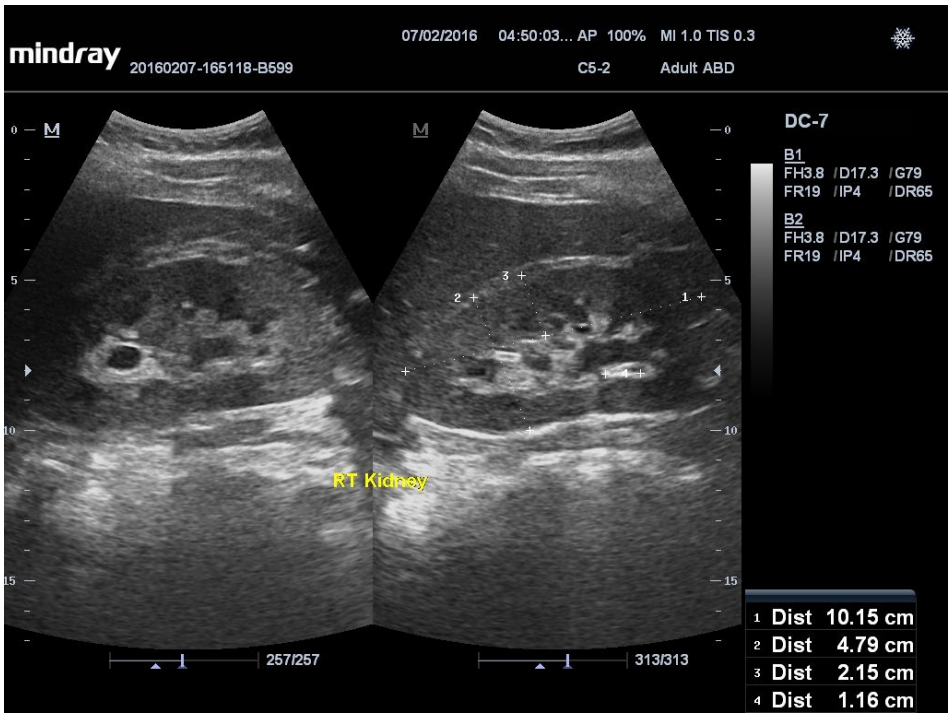

image. (A-27): coronal view of right kidney in a 43-year old female patient with pyelonephritis

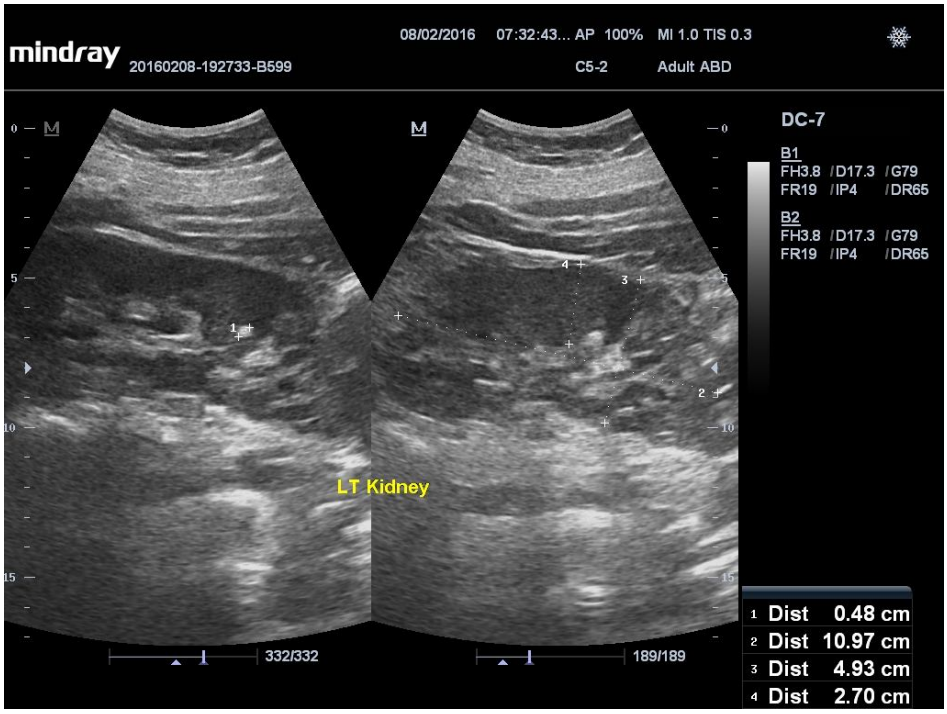

image. (A-28): coronal view of left kidney in a 27-year old male patient with pyelonephritis

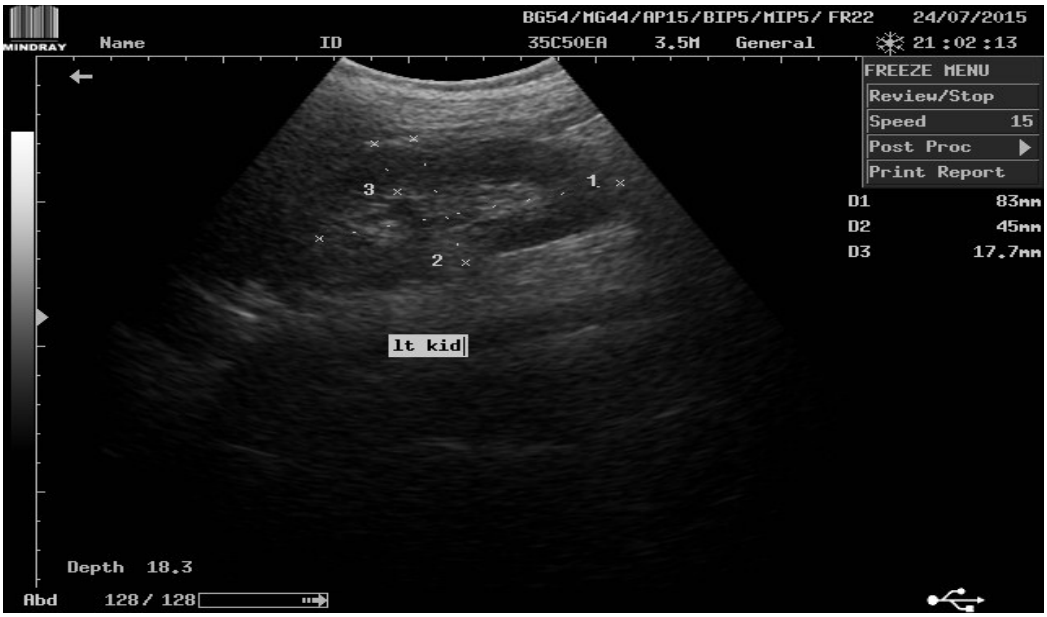

image. (A-29): coronal view of left kidney in a 47-year old female patient with pyelonephritis

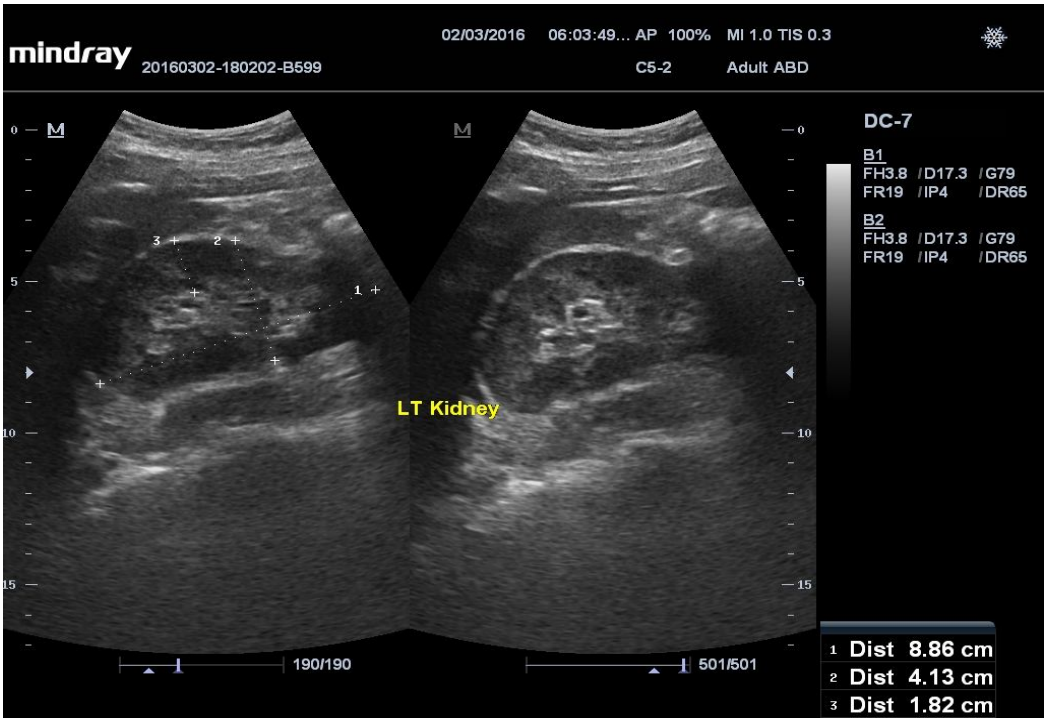

image. (A-30): coronal view of left kidney in a 31-year old female patient with pyelonephritis

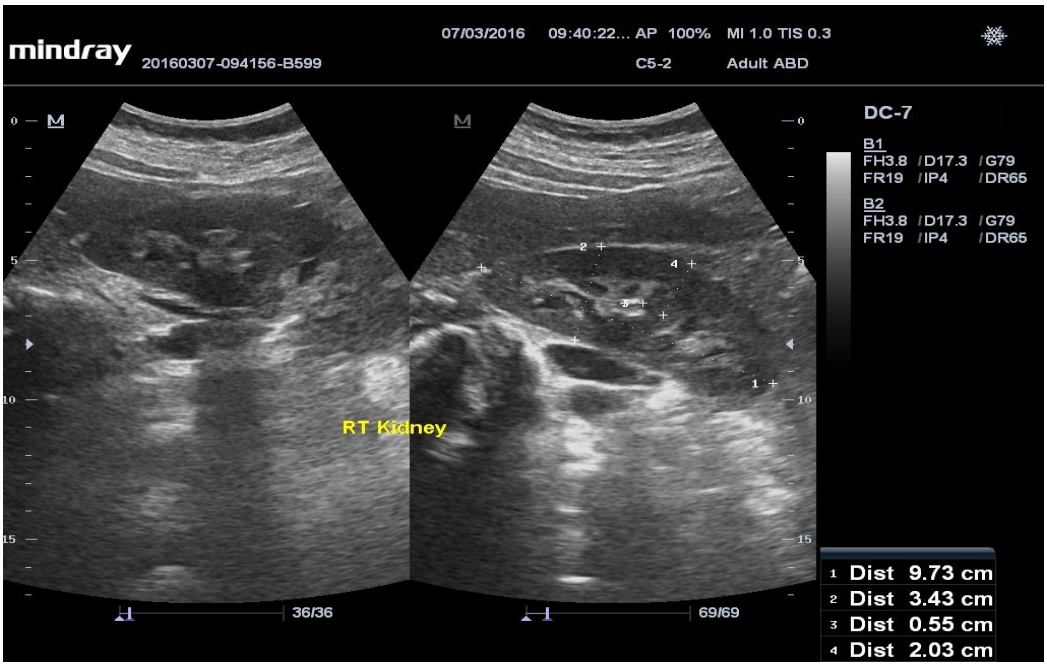

image. (A-31): coronal view of right kidney in a 50-year old male patient with pyelonephritis

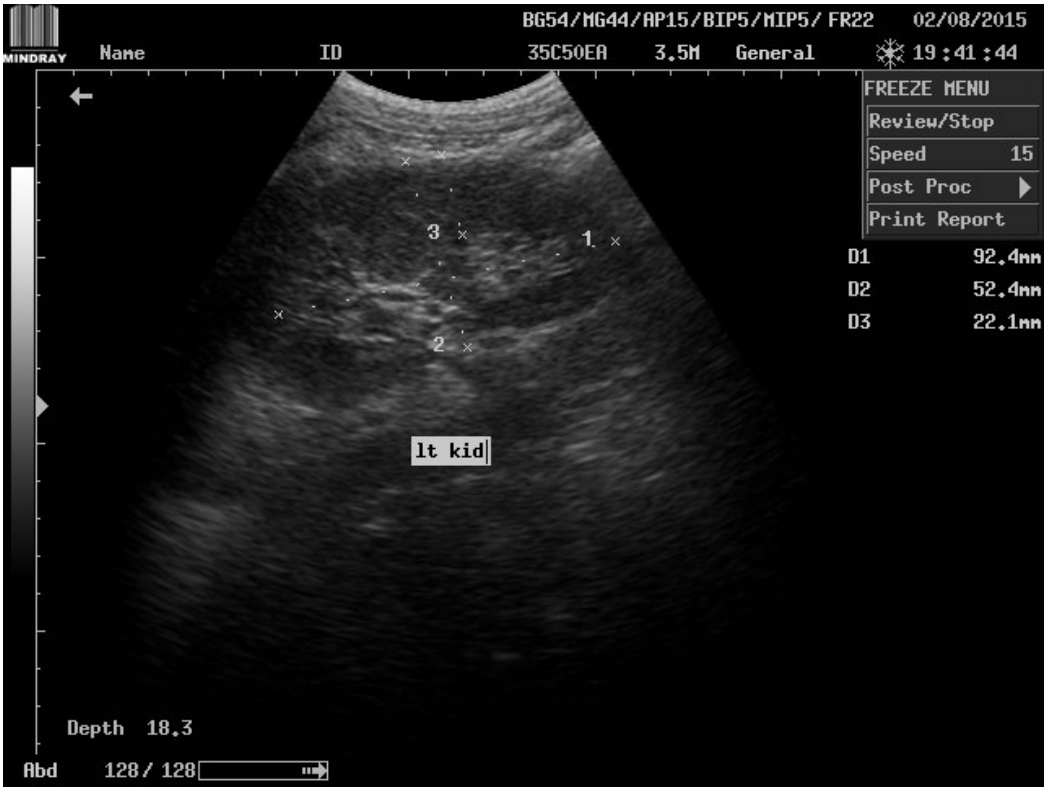

image. (A-32): coronal view of left kidney in a 23-year old female patient with pyelonephritis

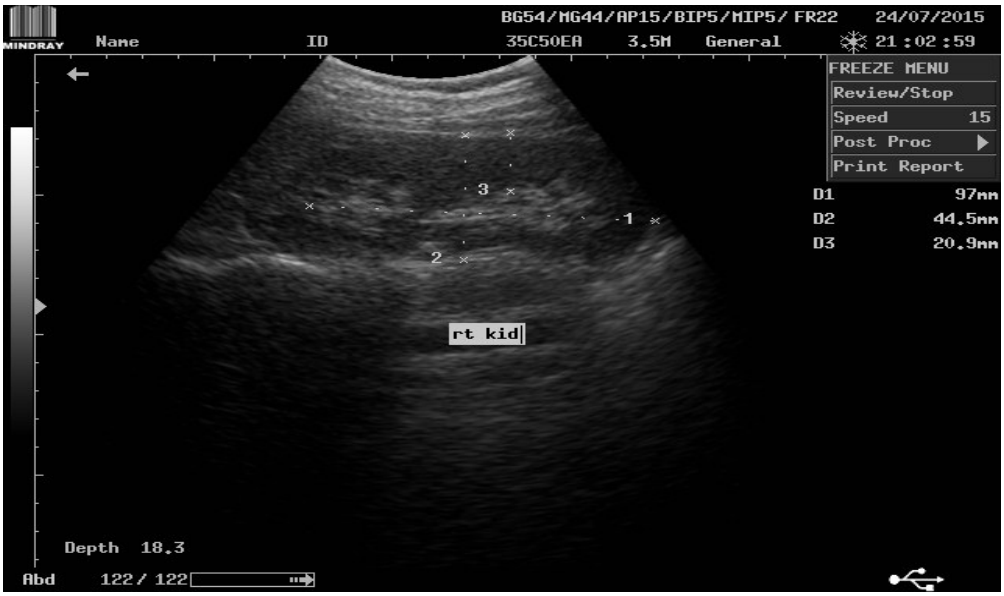

image. (A-33): coronal view of right kidney in a 64-year old male patient with pyelonephritis

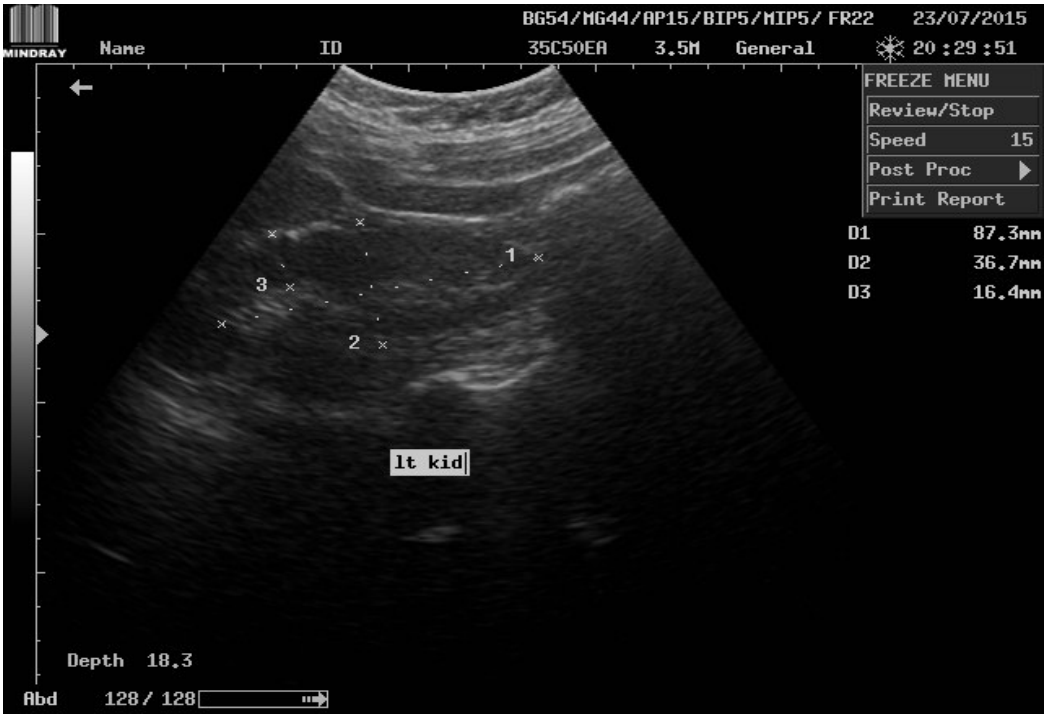

image. (A-34): coronal view of left kidney in a 41-year old female patient with pyelonephritis

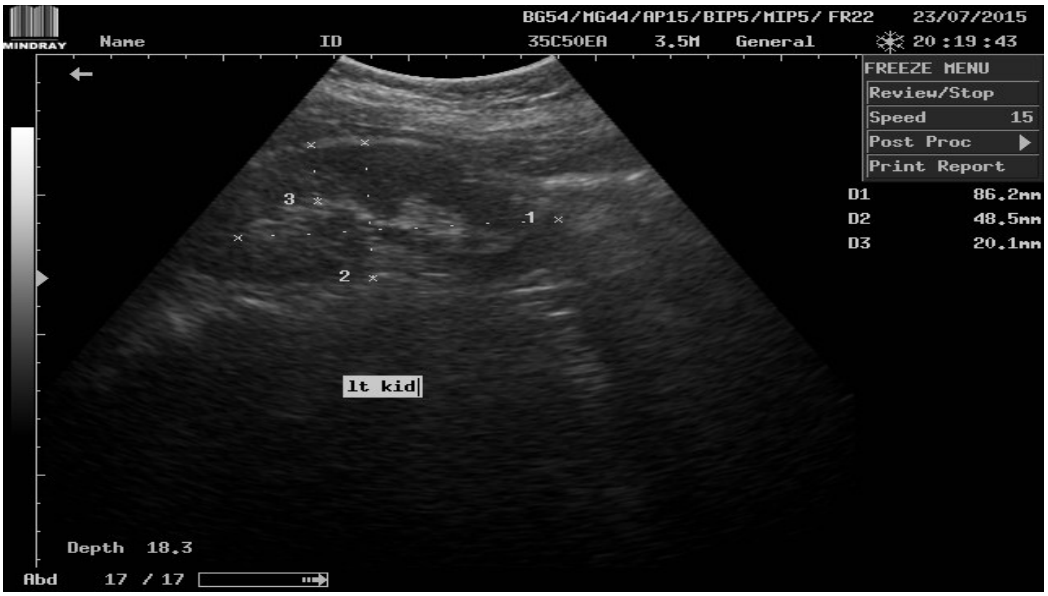

image. (A-35): coronal view of left kidney in a 68-year old female patient with pyelonephritis

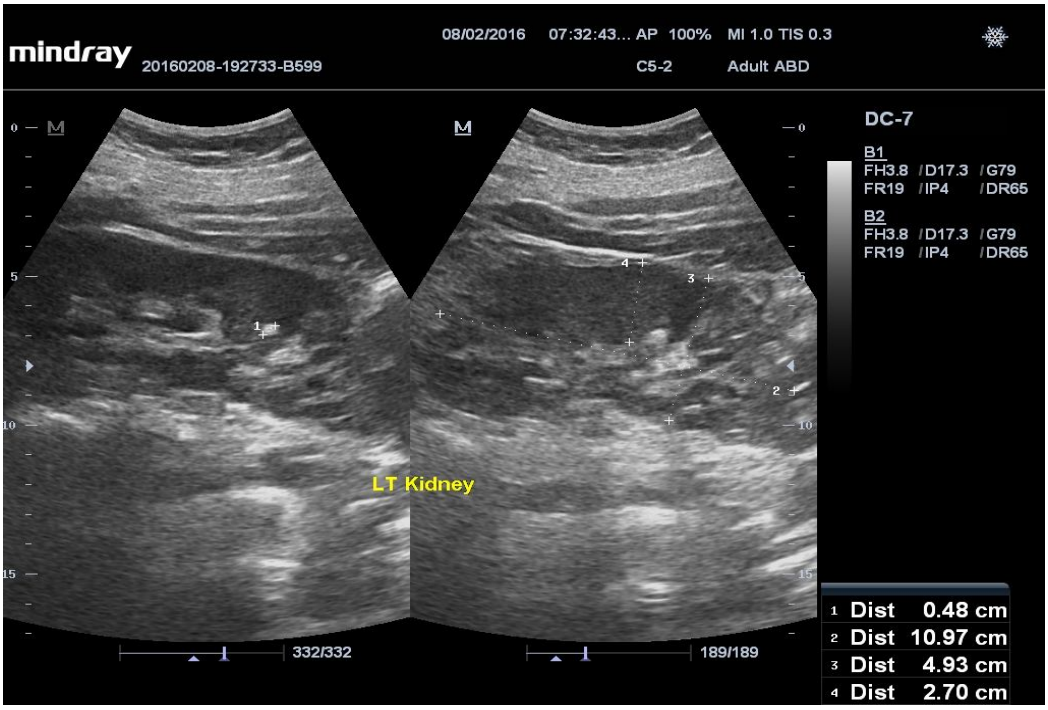

image. (A-36): coronal view of left kidney in a 21-year old female patient with pyelonephritis

Appendix (B)

Published papers